Advancing Alzheimer's disease pharmacotherapy: efficacy of glucocorticoid modulation with dazucorilant (CORT113176) in preclinical mouse models

Canet, G.; Zussy, C.; Vitalis, M.; Morin, F.; Chevallier, N.; Hunt, H.; ... ; Givalois, L.

Received: 27 August 2024 | Revised: 8 November 2024 | Accepted: 24 November 2024

DOI: 10.1111/bph.17457

RESEARCH ARTICLE

Advancing Alzheimer's disease pharmacotherapy: efficacy of glucocorticoid modulation with dazucorilant (CORT113176) in preclinical mouse models

Geoffrey Canet[1,2] | Charleine Zussy[1] | Mathieu Vitalis[1] | Françoise Morin[2] | Nathalie Chevallier[1] | Hazel Hunt[3] | Sylvie Claeysen[4] | Marine Blaquière[4] | Nicola Marchi[4] | Emmanuel Planel[2] | Onno C. Meijer[5] | Catherine Desrumaux[1,6] | Laurent Givalois[1,2,7]

[1]MMDN, Univ Montpellier, EPHE-PSL, INSERM, Montpellier, France

[2]Faculty of Medicine, Department of Psychiatry and Neurosciences, CR-CHUQ, Laval University, Québec City, Quebec, Canada

[3]Corcept Therapeutics, Menlo Park, California, USA

[4]IGF, Univ Montpellier, CNRS, INSERM, Montpellier, France

[5]Einthoven Laboratory, Department of Medicine, Division of Endocrinology, Leiden University Medical Center, Leiden, The Netherlands

[6]LIPSTIC LabEx, Dijon, France

[7]CNRS, Paris, France

Correspondence
Laurent Givalois, Molecular Mechanisms in Neurodegenerative Dementia (MMDN) Laboratory, U1198 INSERM, Team Environmental Impact in Alzheimer's Disease (EiAlz), University of Montpellier, Place E. Bataillon, 34095 Montpellier, France.
Email: laurent.givalois@umontpellier.fr

Geoffrey Canet, Laval University, Faculty of Medicine, Department of Psychiatry and Neurosciences, CR-CHUQ, Québec city (QC), Canada.
Email: geoffrey.canet.1@ulaval.ca

Funding information
Association France Alzheimer & Fédération pour la Recherche sur le Cerveau, Grant/Award Number: SM2016#1512; Fondation pour la Recherche Médicale, Grant/Award Number: MND202003011477-OPA; Agence Nationale de la Recherche, Grant/Award Numbers: ANR-11-LABEX-0021-LipSTIC, ANR-AAP2022-R22102FF-EpiNeurAge; Alzheimer Society of Canada, Grant/Award Number: Postdoctoral fellowship; Université de Montpellier, Grant/Award Numbers: CBS2 PhD program, MUSE-AAP20REC-FRS09-GAiA

Background and Purpose: Exposure to chronic stress and high levels of glucocorticoid hormones in adulthood has been associated with cognitive deficits and increased risk of Alzheimer's disease (AD). Dazucorilant has recently emerged as a selective glucocorticoid receptor (NR3C1) modulator, exhibiting efficacy in counteracting amyloid-β toxicity in an acute model of AD. We aim to assess the therapeutic potential of dazucorilant in reversing amyloid and tau pathologies through the inhibition of glucocorticoid receptor pathological activity, and providing additional evidence for its consideration in AD treatment.

Experimental Approach: The efficacy of dazucorilant was evaluated in two transgenic mouse models of amyloid pathology. The slowly progressing J20 and the aggressively pathological 5xFAD mice. Behavioural analysis was conducted to evaluate welfare, cognitive performances and anxiety levels. The activity of the glucocorticoid receptor system, neuroinflammation, amyloid burden and tau phosphorylation were examined in hippocampi.

Key Results: In both AD models, chronic treatment with dazucorilant improved working and long-term spatial memories along with the inhibition of glucocorticoid receptor-dependent pathogenic processes and the normalization of plasma glucocorticoid levels. Dazucorilant treatment also resulted in a reduction in tau hyperphosphorylation and amyloid production and aggregation. Additionally, dazucorilant

Abbreviations: AD, Alzheimer's disease; APP, amyloid precursor protein; CA1/CA3, Ammon's horn 1 and 3; d-PP2Ac, PP2A catalytic subunit demethylated at Leu309; FAD, Familial Alzheimer's Disease; GFAP, glial fibrillary acidic protein; Iba-1, Ionized calcium-binding adaptor molecule 1; m-PP2Ac, PP2A catalytic subunit methylated at Leu309; oAβ, oligomeric solution of Aβ; qPCR, quantitative polymerase chain reaction; TauC3, tau cleaved at D421; TREM2, Triggering receptor expressed on myeloid cells 2.

seemed to mediate a specific re-localization of activated glial cells onto amyloid plaques in J20 mice, suggesting a restoration of physiological neuroinflammatory processes.

Conclusion and Implications: Dazucorilant exhibited sustained disease-modifying effects in two AD models. Given that this compound has demonstrated safety and tolerability in human subjects, our results provide pre-clinical support for conducting clinical trials to evaluate its potential in AD.

KEYWORDS

5xFAD mice, Alzheimer's disease, Amyloid-β peptide, glucocorticoid receptors, HPA axis, J20 mice, neuroinflammation, Tau protein

1 | INTRODUCTION

Alzheimer's disease (AD) is the leading cause of dementia in the elderly. This neurodegenerative pathology is characterized by a progressive decline in cognitive functions and the presence of senile plaques and neurofibrillary tangles (NFT) throughout the brain, including key regions involved in memory formation and emotional regulation. Senile plaques consist of insoluble extracellular aggregates of **amyloid-β (Aβ)** peptides, while neurofibrillary tangles result from the intraneuronal aggregation of hyper- and abnormally phosphorylated tau protein (Querfurth & LaFerla, 2010; Selkoe & Hardy, 2016). While familial forms linked to specific genetic mutations account for less than 1% of cases, the vast majority of patients (99%) presents with sporadic forms of AD, with unidentified mechanisms but established risk factors (Querfurth & LaFerla, 2010; Selkoe & Hardy, 2016). Besides ageing, growing evidence suggests that environmental and lifestyle factors may increase the susceptibility to develop AD. Significantly, clinical observations reported that stressful life events reduce the onset age of AD (Mejía et al., 2003), while stress-related disorders such as depression may promote AD symptoms and neuropathology (Canet et al., 2018; Canet et al., 2019; Herbert & Lucassen, 2016).

The hypothalamic–pituitary–adrenal (HPA) axis, pivotal for the stress response, triggers the release of glucocorticoids (GC; cortisol in humans and corticosterone in rodents) from the adrenal cortex. These steroid hormones cross the blood–brain barrier and bind to low-affinity glucocorticoid receptors (NR3C1; GR) and high-affinity **mineralocorticoid receptors (NR3C2)**, expressed by neuronal and/or astroglial cells (Reul & de Kloet, 1985). Glucocorticoid are crucial in normal cellular activity and are fundamental for many CNS functions, including learning and memory (Roozendaal, 2000). While mineralocorticoid receptors are predominantly expressed in the hippocampus, glucocorticoid receptors are more ubiquitous, particularly in limbic structures (prefrontal cortex [PFC], hippocampus and amygdala). These structures are strongly involved in cognitive and psychological functions, and part of the neural circuitry controlling the activity of the hypothalamic–pituitary–adrenal (HPA) axis (Jankord & Herman, 2008). Glucocorticoids acting synergistically with excitatory amino acids like **glutamate**, can induce neurotoxicity (McEwen, 2008). Therefore, dysregulation of HPA axis activity and/or alterations in glucocorticoid receptor function may be highly toxic, especially in limbic structures (McEwen, 2008), contributing to the cognitive decline and psychological symptoms observed in AD. In transgenic (Tg) animal models of AD, stress and glucocorticoids administration affect the course of the pathology. For instance, chronic stress and prolonged treatment with glucocorticoids have been shown to accelerate cognitive deficit onset, trigger amyloid precursor protein (APP) misprocessing, amplify plaque pathology, reduce Aβ clearance, increase Aβ levels and promote accumulation of hyperphosphorylated tau (Canet et al., 2022; Green et al., 2006; Rothman et al., 2012). This view is strongly supported by the observation that in AD patients, cognitive and psychological symptoms are linked to an early dysregulation of the HPA axis, increased levels of glucocorticoids in plasma and CSF, as well as impaired glucocorticoid feedback (Csernansky et al., 2006; Hartmann et al., 1997; Hoogendijk et al., 2006). In an acute pathomimetic model of AD induced by a single intracerebroventricular (i.c.v)

What is already known?

- Selective glucocorticoid receptor modulators exhibit neuroprotective properties in experimental models of neurodegenerative disorders.

What does this study add?

- Glucocorticoid receptor-specific modulation by dazucorilant benefits cognition and reduces neuropathology in two AD transgenic models.

What is the clinical significance?

- Selective glucocorticoid receptor modulators in clinical trials show good safety and tolerability for glucocorticoid-associated diseases.

injection of an oligomeric solution of Aβ (oAβ) (Canet, Zussy, et al., 2023; Zussy et al., 2011), we demonstrated a robust and long-lasting activation of the HPA axis, accompanied by altered expression of glucocorticoid and mineralocorticoid receptors in brain regions regulating glucocorticoids secretion (i.e. hippocampus, amygdala and hypothalamus) (Brureau et al., 2013; Pineau et al., 2016). Moreover, our previous results revealed that a one-week treatment with CORT108297 or **dazucorilant (CORT113176)**, acting as selective glucocorticoid receptor modulator, reversed memory deficits, mitigated HPA axis hyperactivity and reduced synaptic impairments, APP misprocessing, neuroinflammation and apoptotic processes induced by the amyloid toxicity in the hippocampus and prefrontal cortex (Canet et al., 2020; Pineau et al., 2016). Altogether, these data strongly support the involvement of the HPA axis in the aetiology of AD.

Here, we aimed to provide additional pre-clinical support for this therapeutic approach in a progressive *in vivo* AD model, using J20 transgenic mice. We focused on the hippocampus given its early and severe vulnerability in AD (Querfurth & LaFerla, 2010) and its regulatory function on PBS axis activity due to high glucocorticoid receptor expression (McEwen, 2008; Reul & de Kloet, 1985). Then, we confirmed the benefits of dazucorilant by evaluating some of the more AD-relevant outcomes in a more aggressive amyloid-producing mouse model, 5xFAD (transgenic mice). We observed in both models that a 4-week chronic treatment protocol with dazucorilant:- (i) improved memory performances and reduced anxiety-like behaviours, (ii) normalized plasma glucocorticoids levels, (iii) inhibited glucocorticoid receptor pathological overactivation and detrimental neuroinflammatory processes and (iv), reduced amyloid production and plaques, as well as **tau** hyperphosphorylation. Our findings collectively underline the therapeutic efficacy and potential disease-modifying effects of dazucorilant, thereby supporting dazucorilant as a viable therapeutic approach for AD.

2 | METHODS

2.1 | Animals

Initially purchased from the Jackson Laboratory and originally produced by L. Mucke (Mucke et al., 2000), adult male J20 mice ($hAPP^{+/+}_{Sw/Ind}$) (*MTA #UM140255-01 with the Gladstone Institute*) ubiquitously overexpress a mutant form of human amyloid precursor protein (hAPP) bearing both Swedish (KM670/671NL) and Indiana (V717F) mutations (APPSwInd), providing a progressive chronic model of AD. We used only male mice in this study to minimize variability associated with hormonal fluctuations during the estrous cycle in females, which can influence glucocorticoid receptor signalling and cognitive functions (Zhang et al., 2009). Further analyses are warranted to confirm these results in female mice, as it has been shown that dazucorilant is less effective in slowing down motor impairment in female mice than in male mice (Gentenaar et al., 2024). These mice were bred in our animal facility (University of Montpellier, CECEMA) under standard conditions (12H/12H light/dark cycle with lights on at 07H00; 21 ± 1°C, food and water *ad libitum*) and were backcrossed >10 generations (Zussy et al., 2022). For breeding, male J20 mice were mated with female C57BL/6 mice (Janvier Lab., France). Wild-type (WT) littermates were used as controls. In order to have a well-established AD pathology, including memory deficits and marked amyloid pathology (Mansuy et al., 2018), 8-month-old male mice were used throughout this study.

The generation of transgenic 5xFAD mice has been described previously (Oakley et al., 2006). These mice carry mutations in both human amyloid precursor protein (APP695) and **presenilinn1 (PSEN1)** genes. The APP gene harbours three Familial Alzheimer's Disease (FAD) mutations:- Swedish (K670N, M671L), Florida (I716V) and London (V717I), and the human *PSEN1* gene harbours two FAD mutations:- M146L and L286V. The 5xFAD strain (B6/SJL genetic background) was maintained by crossing heterozygous transgenic mice with B6/SJL F1 breeders (Jackson Laboratories, Bar Harbour, Maine, USA). F1 male mice resulting from the cross between 5xFAD (B6/SJL) and C57BL/6 mice were further crossed with C57BL/6 female mice and the male offspring was backcrossed more than eight times with C57BL/6 female mice as previously described (Baranger et al., 2016). Wild-type (TW) littermates were used as controls. Given this model exhibits AD-related pathology from 3 months of age (Giannoni et al., 2016; Rochais et al., 2020) and that we aimed to evaluate the curative properties of our treatment, we used 6-month-old male mice throughout this study.

All experiments, including kills, were performed between 09H00 and 14H00, during the diurnal trough of the HPA axis circadian rhythm.

2.2 | Ethical considerations

Animal procedures were conducted in strict adherence to the European Union Directive of 2010 (2010/63/EU) and in compliance with the ARRIVE guidelines (Percie du Sert et al., 2020), and the editorial British journal of pharmacology on reporting animal studies (Lilley et al., 2020). The National French Animal Welfare Committee and the local committee at the University of Montpellier approved all protocols (authorization: APAFIS#35152). All efforts were made to minimize the number of animals used, potential pain, suffering and distress.

2.3 | Experimental procedures and animal groups

Developed by Corcept Therapeutics, dazucorilant belongs to a novel class of selective non-steroidal glucocorticoid receptor ligands (1H-pyrazolo[3,4-g]hexahydro-isoquinoline sulfonamide) with excellent affinity for glucocorticoid receptor and negligible affinity for other nuclear hormone receptors, including **progesterone (NR3C3)**, **androgen (NR3C4)**, mineralocorticoid and **oestrogen (NR3A1/2)** receptors (Beaudry et al., 2014; Pineau et al., 2016). The term selective glucocorticoid receptor modulator reflects its biological properties, as dazucorilant exhibits partial antagonism and some agonism in a transrepression

assay (Gazorpak et al., 2023; Pineau et al., 2016). Importantly, this molecule likely has the potential to selectively block pathogenic glucocorticoid receptor-dependent processes in the brain as an antagonist, while potentially retaining some beneficial aspects of glucocorticoid receptor signalling as an agonist (Meijer et al., 2018; Pineau et al., 2016).

To evaluate the impact of the selective glucocorticoid receptor modulator dazucorilant on Alzheimer's pathology in the J20 and 5xFAD transgenic mouse models, male mice (8 months, n = 7–10 per group for J20 and 6 months, n = 7–9 per group for 5xFAD) were implanted subcutaneously with an osmotic pump (Alzet®, Charles-River, France) that delivered 20 $mg \cdot kg^{-1} \cdot day^{-1}$ of dazucorilant during 4 weeks (Figures 1a and 8a). Animals implanted with an osmotic pump containing vehicle (80% DMSO, 20% sterile 0.9% NaCl) served as control. Mice were anaesthetised with isoflurane (O_2 0.2 $l \cdot min^{-1}$, air 0.2 $l \cdot min^{-1}$ and isoflurane 2%) and after a small incision, the osmotic pump was positioned subcutaneously on the animals flanks. After implantation, the mice were housed individually in transparentcage (Tecniplast, Lyon, France) to promote wound healing and prevent them from removing

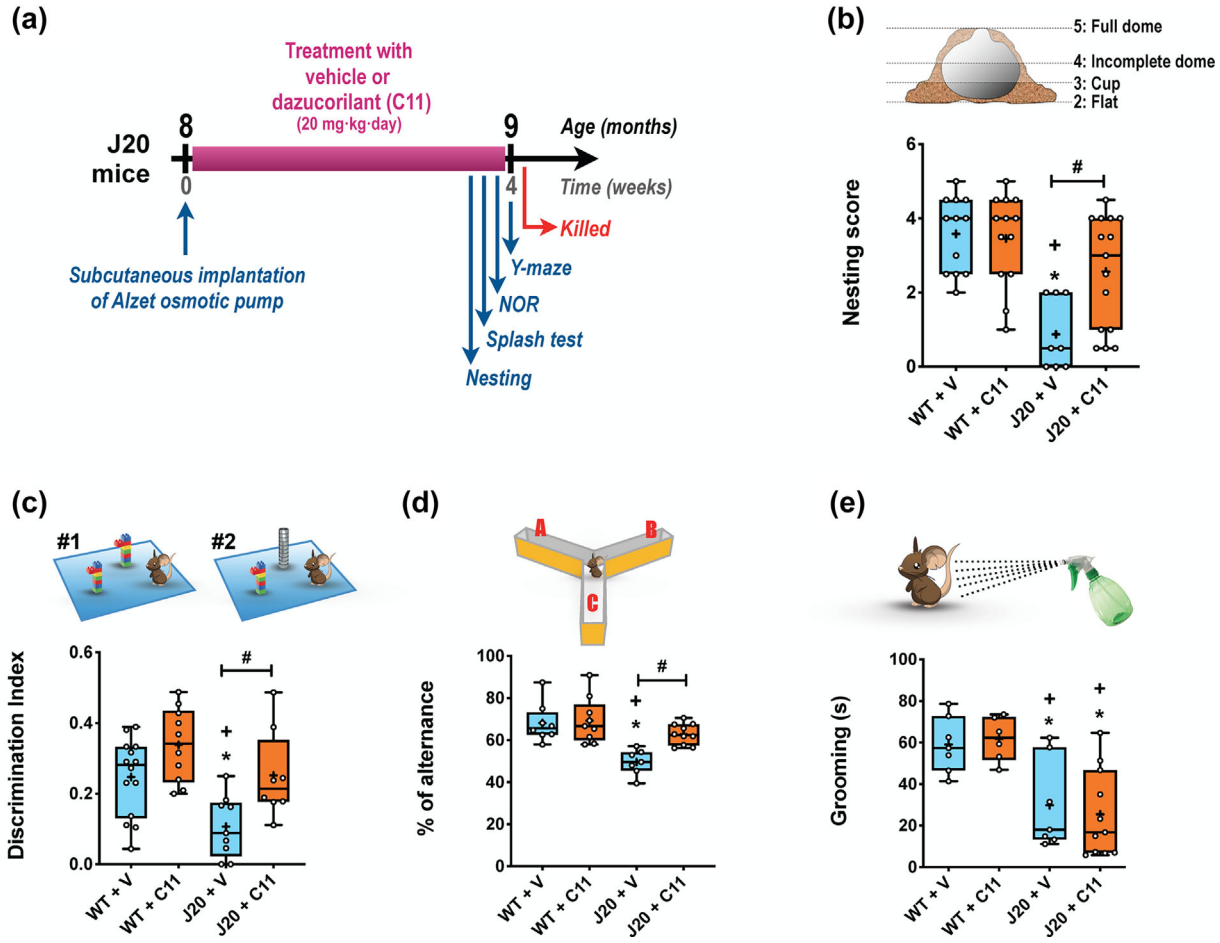

FIGURE 1 Chronic treatment with dazucorilant prevents behavioural impairments in J20 mice. (a) Experimental protocol at T0, at the age of 8 months, J20 mice and wildtype (WT) littermates were subcutaneously implanted with an osmotic micropump (Alzet®) which delivered during 4 weeks 20 $mg \cdot kg^{-1} \cdot day^{-1}$ of dazucorilant (C11) or a vehicle solution (V). At the age of 9 months, the behavioural performances of all mice were tested. (b) Overall welfare behaviour was determined by the nesting test. Nest building was scored according to a rating scale of 1–5 (Hess et al., 2008). A two-way ANOVA followed by a Tukey's multiple comparison were performed: $F_{1,44} = 23.9$ for group ($P < 0.05$); $F_{1,44} = 4.53$ for treatment ($P < 0.05$); and $F_{1,44} = 6.05$ for interaction ($P < 0.05$). * $P < 0.05$ versus WT + V group. + $P < 0.05$ versus WT + C11 group. # $P < 0.05$ versus selected group. (c) Recognition memory was determined using the novel object recognition (NOR) test. The sensitivity of recognition memory was assessed by calculating the preferential discrimination index (Sivakumaran et al., 2018). A two-way ANOVA followed by a Tukey's multiple comparison were performed: $F_{1,38} = 13.1$ for group ($P < 0.05$); $F_{1,38} = 8.69$ for treatment ($P < 0.05$); and $F_{1,38} = 0.13$ for interaction (ns). (d) Spontaneous working memory performance was determined in a Y maze test. The number of arm entries and the number of triads were recorded to calculate the percentage of alternations. A two-way ANOVA followed by a Tukey's multiple comparison were performed: $F_{1,30} = 19.9$ for group ($P < 0.05$); $F_{1,30} = 6.61$ for treatment ($P < 0.05$); and $F_{1,30} = 4.63$ for interaction ($P < 0.05$). (e) The anxious/depressive behaviour was determined using the splash test (David et al., 2009). A 10% sucrose solution was sprayed onto the dorsal coat of mice and the grooming frequency was recorded for 5 min. A two-way ANOVA followed by a Tukey's multiple comparison were performed: $F_{1,27} = 24.2$ for group (* $P < 0.05$); $F_{1,27} = 0.02$ for treatment (ns); and $F_{1,27} = 0.28$ for interaction (ns). * $P < 0.05$ versus WT + V group. + $P < 0.05$ versus WT + C11 group. # $P < 0.05$ versus selected group. All data are presented as box and whiskers with min to max and median adn n = 6-14 mice per group. ns: non-significant.

each other's sutures. From 3 weeks after the implantation of the osmotic pumps containing selective glucocorticoid receptor modulator (dazucorilant) or vehicle, behavioural tests (Nesting, Splash, novel object recognition and/or Y maze tests) were performed to characterize the impact of the treatment on Alzheimer's pathology. All tests were conducted in a dedicated room and the animals were placed in this room at least 30 min before each test. Videotaped data were analysed with the 'Ethovison' software (Noldus). To minimize stress and avoid subjecting mice to multiple behavioural tasks, we divided the tests among different batches of mice. The sporadic occurrence of eyelid dermatitis was used as an exclusion criterion, as it could impact the mice's motivation and performance during behavioural tests. However, if these mice were otherwise healthy, they were included in post-mortem analyses.

One day after the end of behavioural tests (i.e. 4 weeks after the implantation of the osmotic pump), a subset of mice (n = 5 per group) was anaesthetised with an i.p. injection of a mixture of ketamine (100 mg·kg^{-1})/xylazine (10 mg·kg^{-1}) and perfused intracardially with NaCl buffer (0.9%) for exsanguination, and then with a 4% paraformaldehyde solution until tissue fixation. The brains were carefully removed for histological and immunohistochemical analysis. The other subsets of mice were killed by decapitation without anaesthesia, as anaesthesia leads to tau hyperphosphorylation (Canet, Rocaboy, et al., 2023). For each animal, death was confirmed by the absence of a heartbeat and respiration before proceeding with tissue collection. Blood samples were collected for corticosterone assay and the hippocampi were rapidly dissected, and randomly allocated to ELISA, western blot or qPCR analyses.

2.4 | Behavioural tests

All behavioural analyses and quantifications were performed in a blinded manner.

2.4.1 | Welfare behaviour (nesting)

In rodents, nest-building is a species-specific form of active interaction with the environment for shelter and temperature regulation. Both male and female mice build a nest when they are provided with suitable building material. This method aims to exploit highly motivated nesting behaviours to quickly characterize the animal's overall welfare, which is affected by the amyloid pathology (Mansuy et al., 2018). Mice were individually housed on sawdust in standard cages and a 5 × 5-cm cotton piece was introduced into each cage approximately 3 h before the onset of the dark phase. The next morning, nest building behaviour was scored according to a previously described rating scale of 1–5 (Figures 1b and 8b) (Hess et al., 2008).

2.4.2 | Long-term recognition memory

The novel object recognition (NOR) test is a highly validated test for recognition memory in mice. The test relies on three sessions (habituation, training and test) and can be completed over 2 days (Figures 1c and 8c). Mice were placed individually in a circular open field (50 cm in diameter) made in Plexiglas, with a floor equipped with infrared light-emitting diodes. The first day of trial, mice were habituated to the arena for 10 min (Session 1). One hour later (Session 2—training session), mice explored two identical objects (plastic bricks of construction game) placed at defined positions of one diagonal of the arena for 10 min. The next day (Session 3—test session), one of the familiar objects was replaced with a novel one (graduated glass cylinder) differing in colour, shape and texture, and mice explored for 10 min. The preferential discrimination index, indicative of recognition memory sensitivity (Sivakumaran et al., 2018), was calculated as follows:- (number of contacts with the novel object − number of contact with the familiar object)/total contacts number. The exploratory activity of each mouse during Sessions 2 and 3 were recorded using the Noldus EthoVisonXT video-tracking system.

2.4.3 | Short-term memory (Y maze)

The Y maze spontaneous alternation was used to assess short term memory in mice. Spontaneous alternation (spatial working memory) can be assessed by allowing mice to explore all three arms (Figures 1d and 8d) of the maze and is driven by an innate curiosity of rodents to explore previously unvisited areas. After introduction to the centre of the maze, the animal was allowed to freely explore the three arms during 8 min (Mansuy et al., 2018). The number of arm entries and the number of triads was evaluated to calculate the percentage of alternation using the Noldus EthoVisonXT video-tracking system.

2.4.4 | Anxious/depressive like behaviour (splash test)

The splash test consists of spraying a 10% sucrose solution on the dorsal coat of a mouse (David et al., 2009). Due to its viscosity, the sucrose solution dirties the coat and induces a grooming behaviour (Figure 1e). The grooming frequency was recorded for 5 min as an index of self-care and motivational behaviour that could be considered to parallel with some symptoms of anxiety/depression such as apathetic behaviour (David et al., 2009).

2.5 | Corticosterone and human Aβ_{1-42} assays

Blood samples were collected after the mice had been killed through decapitation without anesthesia (BD vacutainer® EDTA), centrifuged at 4°C and plasma was stored at −20°C until corticosterone assay (Canet et al., 2020; Canet et al., 2022). Plasma corticosterone concentrations were determined using a conventional ELISA kit (ARBOR Assays, USA) in a 5-µl plasma sample diluted (1:100) with the assay buffer. Assay sensitivity was 17.5 pg·ml^{-1}. Intra- and inter-assay coefficients were 5.2% and 7.9%, respectively. Human amyloid-β (1-42) peptide was quantified

in soluble and insoluble fractions of hippocampal homogenates using ELISA kit (Human Aβ42 Ultrasensitive ELISA Kit, Invitrogen) (Mansuy et al., 2018). Briefly, 2% sodium dodecyl sulphate (SDS) was added to brain homogenates prior to ultracentrifugation at 19,600×*g* for 30 min at 4°C. The resulting supernatants were collected to quantify the soluble fractions of human $A\beta_{1-42}$ peptides, while the pellets were used to quantify the insoluble fraction. Results were normalized against protein concentrations calculated using the bicinchoninic acid method (BCA kit, ThermoFisher Scientific, France). Assay sensitivity was 1 pg·ml^{-1}. Intra- and inter-assay coefficients were 8.6% and 7.5%, respectively.

2.6 | Histology and immunohistochemistry analysis

Harvested brains were postfixed in a 4% paraformaldehyde solution for 48 h (4°C) and then in a sucrose solution (30%) for 3 days (4°C). Thereafter, the tissues were embedded in a block of OCT compound (Tissue-Tek, Sakura Finetek, USA) and quickly frozen in chilled acetone on dry ice. Frozen brains were mounted on a cryostat (Leica CM3050-S, France), serially cut into 10-µm coronal sections and mounted on Superfrost® Plus glass (Microm Microtech, France). Slides were acquired and analysed using a Leica DM4B microscope coupled with the Thunder Imager technology (Leica, France). This technology removes the out-of-focus blurring thanks to an optodigital and automated method called 'Computational Clearing System' developed by Leica (Leica Thunder Imaging Systems). The investigator was blinded to the identity of the mouse brains and at least 10 sections were studied from each brain, taken from the anterior hippocampus level (coordinate from bregma: −1.94 mm), with intervals of 10 µm.

Amyloid plaques were quantified according to our previously published protocol (Mansuy et al., 2018). Briefly, slides were rinsed with PBS (0.1 M) to remove cryoprotectants and dehydrated in successive baths of 70% and 80% ethanol. Sections were incubated for 15 min at room temperature with 1% thioflavin S (ThS, resuspended in 80% ethanol), a fluorescent dye used to stain amyloid plaques (Mansuy et al., 2018). Sections were then progressively rehydrated and counterstained with 4′,6′-diamino-2-phenylindole (***DAPI***) to visualize nuclei. The number and the surface area of amyloid aggregates throughout the hippocampus were analysed using Fiji software (NIH, USA). All data per animal were pooled to get the total number and total surface area of aggregates, and then normalized to the total surface area of the hippocampus analysed for each animal.

Analyses of glial (glial fibrillary acidic protein [GFAP]), microglial (ionized calcium-binding adaptor molecule [1Iba-1]), amyloid plaques (6E10) and glucocorticoid receptor protein were conducted using a fluorescent immunohistochemistry approach (Brureau et al., 2013; Mansuy et al., 2018; Zussy et al., 2011; Zussy et al., 2013). All antibodies used are detailed in Table S1. Sections were incubated overnight at room temperature with primary antibodies in a humid chamber and then for 2 h with appropriate fluorescent secondary antibodies (Alexafluor-488 for anti-GFAP, anti-glucocorticoid receptor and anti 6E10 or Cy3 for anti-Iba1 or anti-NeuN) (Invitrogen, Molecular Probes, The Netherlands). The nuclei of all sections were counterstained with 4′,6′-diamino-2-phenylindole (DAPI, Molecular Probes). In the case of 6E10, sections were pretreated with a demasking solution of formic acid (70%) for 15 min at room temperature before immunohistochemistry procedures (Mansuy et al., 2018). Immunostaining specificity was determined by incubating control sections with the secondary antiserum alone.

As previously described (Brureau et al., 2013), to determine the nuclear localization of glucocorticoid receptor, the overlap area of glucocorticoid receptor labeling with the DAPI signal in the regions of interest (CA1, CA3 and hilus) was determined using the FIJI BIOP plugin 'JACoP' developed by Bolte and Cordelières (Bolte & Cordelières, 2006). The overlap area was obtained from the overlap coefficient introduced by Manders et al., and based on the Pearson's correlation coefficient (Manders et al., 1992). Data per section (∼*10 per animal*) were expressed as a percentage of total glucocorticoid receptor labelling and then averaged to get the nuclear localization of glucocorticoid receptor per animal. With this approach, the normalization factor is not dependent on the relative intensities of the green and blue fluorescent signals, or on the gain settings of the microscope's photodetectors (*for more details, see* https://imagej.net/plugins/jacop).

The specific intensity of GFAP or Iba1 immunosignal in senile plaques (labelled with 6E10) was calculated as the ratio of the signal intensity of each marker (GFAP or Iba1) present on senile plaques to the total signal intensity determined for each acquired image (maintaining constant exposure for all samples across a single experiment). Data per section (∼10 per animal) were averaged to obtain the relative intensity of each marker (GFAP or Iba1) at the level of senile plaques per animal.

2.7 | Western blot analysis

The Immuno-related procedures used comply with the recommendations made by the *British Journal of Pharmacology* (Alexander et al., 2018). Western blots were performed as previously described (Canet et al., 2022; Zussy et al., 2011) in the hippocampus. All antibodies used are detailed in Table S1. Briefly, after sacrifice, hippocampi were micro-dissected, weighed, immediately frozen in liquid nitrogen and stored at −20°C. Tissues were sonicated (VibraCell; Sonics & Materials, USA) in a lysis buffer and centrifuged (4°C). Supernatants were collected and protein concentration was measured using a BCA kit (ThermoFisher Scientific). Sixty µg from each sample were used for western blot analysis. Samples were separated in a sodium dodecyl sulphate (SDS)-polyacrylamide gel (12%) and transferred to a PVDF membrane (Merck-Millipore, France). The membrane was incubated overnight (4°C) with appropriate primary antibody, rinsed and then incubated for 2 h with the appropriate horseradish peroxidase-conjugated secondary antibody (Sigma-Aldrich). Peroxidase activity was revealed using enhanced-chemiluminescence (ECL) reagents (Luminata-Crescendo, Merck-Millipore) and quantified using Image-J software (NIH, Bethesda, MA, USA). β-tubulin served as a loading control for all immunoblotting experiments. All western blot quantifications were performed in a blinded manner to ensure objectivity. Due to technical

issues such as sample loss or depletion during experimental procedures, some discrepancies in sample sizes occurred among different biochemical analyses. Two representative lanes from the immunoblots are shown for each specific experimental condition. Brightness levels were adjusted as necessary to enhance visualization and accuracy.

2.8 | RT-qPCR

RT-qPCR were performed as previously described (Zub et al., 2019) in the hippocampus. Tissues were suspended in 350 µl RLT Plus buffer (Qiagen) supplemented with 1% β-mercaptoethanol and lysed within Lysing Matrix D tube into the FastPrep® sample preparation system (MP Biomedicals). Tissue lysate was homogenized on QIAshredder columns (Qiagen). Total cellular RNA was extracted using the RNeasy Mini RNA isolation kit (Qiagen) and genomic DNA contamination was removed using RNase-Free DNase Set (Qiagen). The RNA concentration of each sample was measured with a Nanodrop 2000c spectrophotometer (Thermo Fisher Scientific). Following the manufacturer's instructions, one microgram of total RNA was reverse-transcribed using random hexamers of the Transcriptor First Strand cDNA Synthesis Kit (Roche). RT-qPCR was performed using a 5-µl volume of 10 ng cDNA, 500 nmol·L^{-1} of forward and reverse primers, and 2.5 µl of SYBR Green PCR Master Mix (Roche) in duplicate. The programme ran 45 cycles of denaturation at 95°C for 10 s, annealing at 60°C for 10 s and elongation at 72°C for 15 s, performed in a LightCycler 480 apparatus (Roche). After amplification, the melting curve was assessed to ensure a single product. Each plate carried serial dilutions of an RNA calibrator to generate a standard curve of the efficiency of the primer during the run. The levels of cDNA were quantified by the comparative 2ΔΔCt method. Ct values of the target gene were normalized with the Ct values of the house-keeping gene *GAPDH* (glyceraldehyde 3-phosphate dehydrogenase). Each target value is expressed as n-fold differences relative to the experimental control. Table S2 provides a list of all primers used.

2.9 | Data and statistical analysis

The data and statistical analysis comply with the recommendations on experimental design and analysis in pharmacology (Curtis et al., 2022). Data are presented as box and whiskers (min to max), including the median value. Each data point represents an independent animal and statistical analyses were conducted with group sizes of at least n = 5. Before each analysis of variance, the Gaussian distribution was evaluated and validated by a Kolmogorov–Smirnov test (GraphPad-Prism 9.0). Non-parametric tests (Mann–Whitney & Dunn's) were used when the distribution was not normal. Two- or one-way ANOVA followed by Tukey's multiple comparison tests were used for the normally distributed data sets (*GraphPad-Prism 9.0*). $P < 0.05$ was considered significant. The number of animals and statistical details are indicated in the figure legends. Statistical power analysis was calculated using G*Power.

2.10 | Materials

Dazucorilant was provided by Corcept Therapeutics (Menlo Park, CA, U.SA.), while isoflurane, ketamine and xylazine were purchased from Centravet (Lapalisse, France). DMSO, NaCl, paraformaldehyde, sucrose, ThioflavinS, ethanol and PBS were purchased from Sigma-Aldricht (St. Quentin Fallavier, France). Sodium Dodecyl Sulphate (SDS) was purchased from Euromedex (Souffelweyersheim, France), while 4',6'-diamino-2-phenylindole (DAPI) was purchased from Life-Technologies (Villebon sur Yvette, France).

Details of other materials and suppliers are provided in the specific sections.

2.11 | Nomenclature of targets and ligands

Key protein targets and ligands in this article are hyperlinked to corresponding entries in the IUPHAR/BPS Guide to PHARMACOLOGY http://www.guidetopharmacology.org and are permanently archived in the Concise Guide to PHARMACOLOGY 2023/24 (Alexander, Cidlowski, et al., 2023; Alexander, Fabbro, et al., 2023).

3 | RESULTS

3.1 | Chronic treatment with dazucorilant prevents cognitive impairments in J20 mice

Our previous work in the acute oAβ model of AD demonstrated that a one-week treatment with dazucorilant improved memory deficits and AD-related hallmarks (i.e. APP misprocessing, neuroinflammation and apoptotic processes), along with restoring the HPA axis hormone levels (Canet et al., 2020; Canet, Zussy, et al., 2023; Pineau et al., 2016). Encouraged by these initial findings, we designed and validated a chronic treatment protocol with dazucorilant in 8-month-old J20 mice (Figure 1a), a stage with advanced AD pathology. This murine AD model replicates key features of the disease, including amyloid burden with overproduction of Aβ peptides, accumulation of senile plaques and amyloid vascular deposits, as well as tau hyperphosphorylation, neuroinflammation and cognitive deficits (Dávila-Bouziguet et al., 2019; Mansuy et al., 2018; Mucke et al., 2000). J20 mice and WT littermate controls were treated with a daily dose of 20 mg·kg^{-1} of dazucorilant or vehicle solution for 4 weeks, administered via subcutaneous osmotic micropumps. At the end of treatment, we conducted a behavioural analysis which revealed that dazucorilant treatment in J20 mice restored normal nesting behaviour, indicating improved welfare (Figure 1b). Moreover, in J20 mice, dazucorilant significantly enhanced memory performances in novel object recognition (Figure 1c) and Y maze (Figure 1d) paradigms. However, we did not observe any improvement in grooming behaviour during the splash test in J20 mice following dazucorilant treatment (Figure 1e). Importantly, chronic treatment with dazucorilant in WT mice did not elicit any observable spontaneous behavioural changes (Figure 1b–e).

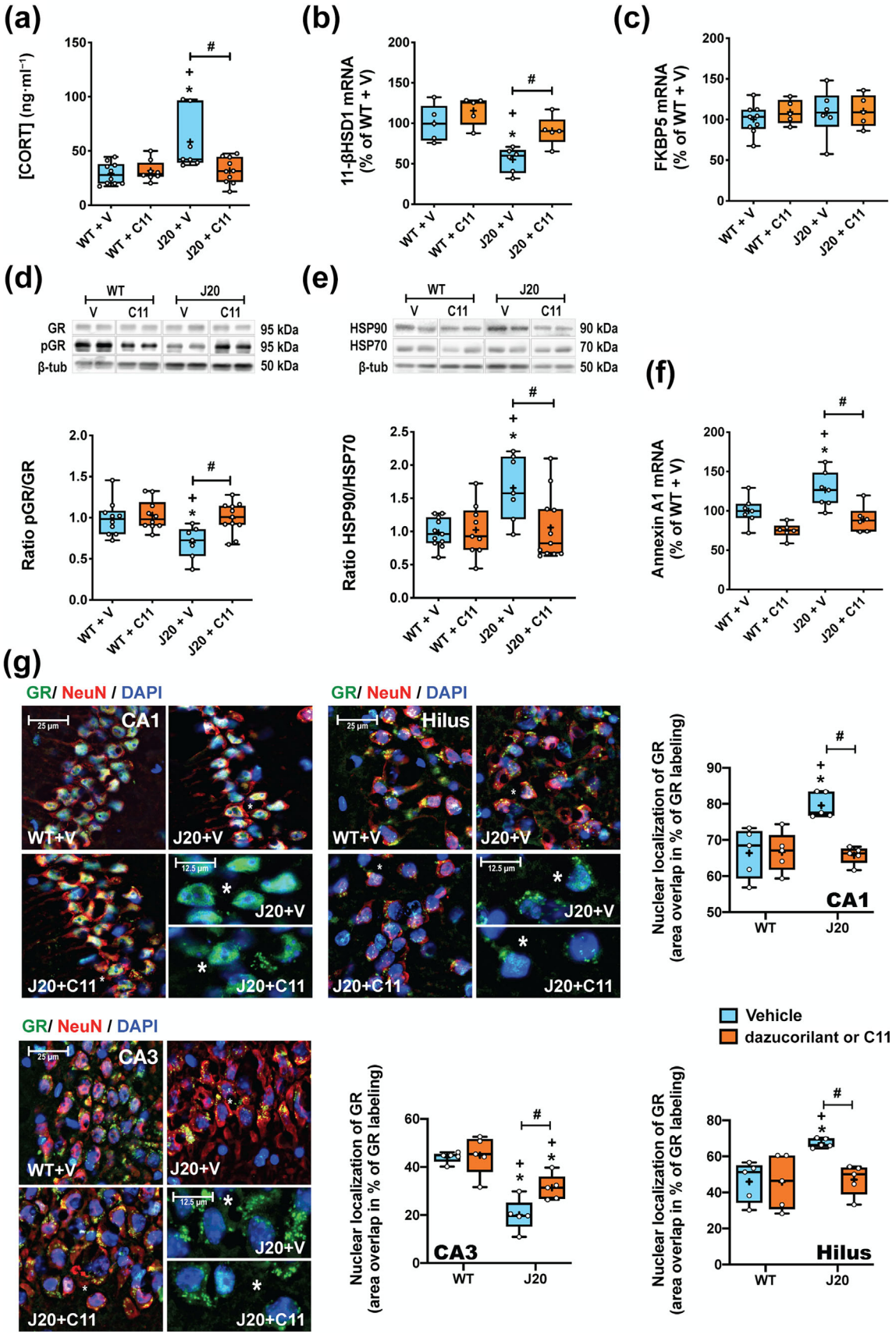

FIGURE 2 Legend on next page.

3.2 | Chronic treatment with dazucorilant normalizes the HPA axis activity and the neuronal localization of glucocorticoid receptor in J20 mice

Chronic administration of dazucorilant restored numerous HPA axis-related physiological parameters, as plasma corticosterone levels (Figure 2a), hippocampal expression of the **11-βHSD1** mRNA (hydroxysteroid 11-beta dehydrogenase 1 or the dehydrocorticosterone-to-corticosterone converting enzyme) (Chapman & Seckl, 2008) (Figure 2b), active phosphorylated form of glucocorticoid receptor (Ser211, pglucocorticoid receptor) (Figure 2d) and the ratio of **HSP90/HSP70** (Figure 2e) (both reflecting the activity level of glucocorticoid receptor) were comparable to the levels observed in WT littermates. In contrast, hippocampal expression of ***Fkbp5*** mRNA (a chaperone regulating glucocorticoid receptor sensitivity but also a glucocorticoid receptor target gene; *Nr3C1*) (Petta et al., 2016) was unaffected by J20 genotype and selective glucocorticoid receptor modulator treatment (Figure 2C). Finally, we observed that administration of dazucorilant in J20 mice reversed the increase in **annexin A1 (ANXA1)** mRNA expression (Figure 2f), coding for an endogenous effector released by immune cells upon glucocorticoid receptor activation which mediates anti-inflammatory actions of glucocorticoids (Perretti & D'Acquisto, 2009). Interestingly, immunohistochemistry analysis revealed a notable glucocorticoid receptor accumulation in the nuclei of hippocampal CA1 and hilus neurons in J20 mice (Figure 2g), consistent with our previous findings in the acute oAβ model of AD (Brureau et al., 2013). Conversely, in the CA3 region, nuclear localization of glucocorticoid receptor was less pronounced in J20 mice than in WT mice (Figure 2g). However, in both cases, dazucorilant administration restored the physiological subcellular localization of glucocorticoid receptor. Collectively, these results suggest revealed several disease model effects related to the disturbed glucocorticoid receptor-associated signalling pathways in J20 mice, all normalized by chronic administration of dazucorilant.

3.3 | Chronic treatment with dazucorilant reduces amyloid load in soluble and insoluble hippocampal fractions of J20 mice

Chronic treatment with dazucorilant of 8-month-old J20 mice, known to exhibit amyloid plaques in the hippocampus (Dávila-Bouziguet et al., 2019; Mansuy et al., 2018; Mucke et al., 2000), had no significant impact on the number of amyloid plaques compared with vehicle-treated J20 mice (Figure 3a,b). However, a significant reduction in plaque size was observed (Figure 3a,c). In a distinct set of experiments, quantification of Aβ_{1-42} levels in soluble and insoluble fractions from hippocampal extracts demonstrated a significant decrease in both fractions following dazucorilant treatment (Figure 3d,e). This effect may be attributed to the concurrent inhibition of key enzymes involved in amyloidogenic pathways and Aβ production (Figure 3f–h). Specifically, hippocampal levels of the main β-secretase component, **BACE1** (β-APP cleaving enzyme) (Figure 3f), as well as of the α-secretases **ADAM10** (Figure 3g) and **ADAM17** (Figure 3h), were normalized in J20 mice treated with dazucorilant. Notably, while counterintuitive the increase in ADAM10 and ADAM17 expressions observed in vehicle-treated J20 mice has been reported in AD patients (Oliveira Monteiro et al., 2021).

3.4 | Chronic treatment with dazucorilant restores levels of rho-associated coiled-coil kinases in the hippocampus of J20 mice

We investigated the impact of dazucorilant treatment on the Rho-associated coiled-coil containing kinase 1 and 2 (ROCK1 and ROCK2)/**3-phosphoinositide-dependent kinase 1 (PDK1)** system, regulated by glucocorticoid receptor (Canet et al., 2022; Rubenstein et al., 2007) and involved in the pathophysiology of AD, particularly

FIGURE 2 Chronic treatment with dazucorilant (C11) normalizes the HPA axis activity and the neuronal localization of glucocorticoid receptor (GR) in J20 mice. For experimental protocol see Figure 1a. (a) Plasma concentrations of corticosterone (CORT) were determined by ELISA and expressed as ng/ml. Two-way ANOVA: $F_{1,33} = 5.67$ for group ($P < 0.05$); $F_{1,33} = 5.44$ for treatment ($P < 0.05$); and $F_{1,33} = 3.65$ for interaction (ns). (b,c) Hippocampal expression of 11-βHSD1 and FKBP5 mRNAs was determined by q-PCR and expressed in % of mRNA levels determined in WT mice treated with the vehicle (WT + V). A two-way ANOVA followed by a Tukey's multiple comparison were performed. For 11-βHSD1 mRNA: $F_{1,17} = 18.7$ for group ($P < 0.05$); $F_{1,17} = 10.1$ for treatment ($P < 0.05$); and $F_{1,17} = 1.55$ for interaction (ns); and for FKBP5 mRNA: $F_{1,21} = 0.28$ for group (ns); $F_{1,21} = 0.44$ for treatment (ns); and $F_{1,21} = 0.15$ for interaction (ns). (d,e) The hippocampal variations of the ratios of pGR/GR (p[Ser211]GR, 95 kDA), HSP90/HSP70 (90 and 70 kDa, respectively), were determined by western blot, normalized with the variations of β-tubulin (β-tub, 55 kDa). A two-way ANOVA followed by a Tukey's multiple comparison were performed. For pGR/GR: $F_{1,34} = 6.30$ for group ($P < 0.05$); $F_{1,34} = 7.024$ for treatment ($P < 0.05$); and $F_{1,34} = 3.92$ for interaction ($P < 0.05$), and for HSP90/HSP70: $F_{1,34} = 6,89$ for group (* $P < 0.05$); $F_{1,34} = 4.26$ for treatment ($P < 0.05$); and $F_{1,34} = 5.94$ for interaction ($P < 0.05$). (f) Hippocampal expression of annexin A1 mRNAs was determined by q-PCR and expressed in % of mRNA levels determined in WT mice treated with the vehicle (WT + V). A two-way ANOVA followed by a Tukey's multiple comparison were performed. $F_{1,17} = 18.7$ for group ($P < 0.05$); $F_{1,17} = 10.1$ for treatment ($P < 0.05$); and $F_{1,17} = 1.55$ for interaction (ns); (g) the quantification of relative nuclear localization (*DAPI staining in blue*) of GR (*in green*) was determined by immunohistochemistry in the hippocampal neurons (*NeuN positive cells in red*) from CA1, CA3 and hilus subregions, and analysis was blindly performed. The nuclear localization of GR was expressed as the area of overlap in % of total GR labelling (cf. *Section 2 for further details*). A two-way ANOVA followed by a Tukey's multiple comparison were performed for each hippocampal subregion. For CA1: $F_{1,16} = 7.77$ for group ($P < 0.05$); $F_{1,16} = 9.52$ for treatment ($P < 0.05$); and $F_{1,16} = 10.1$ for interaction ($P < 0.05$); for CA3: $F_{1,16} = 48.1$ for group ($P < 0.05$); $F_{1,16} = 5.06$ for treatment ($P < 0.05$); and $F_{1,16} = 3.75$ for interaction (ns), and for hilus: $F_{1,16} = 5.99$ for group ($P < 0.05$); $F_{1,16} = 4.82$ for treatment ($P < 0.05$); and $F_{1,16} = 4.67$ for interaction ($P < 0.05$). * $P < 0.05$ versus WT + V group. + $P < 0.05$ versus WT + C11 group. # $P < 0.05$ versus selected group. All data are presented as box and whiskers with min to max and median and n = 5-11 mice per group. ns: non-significant.

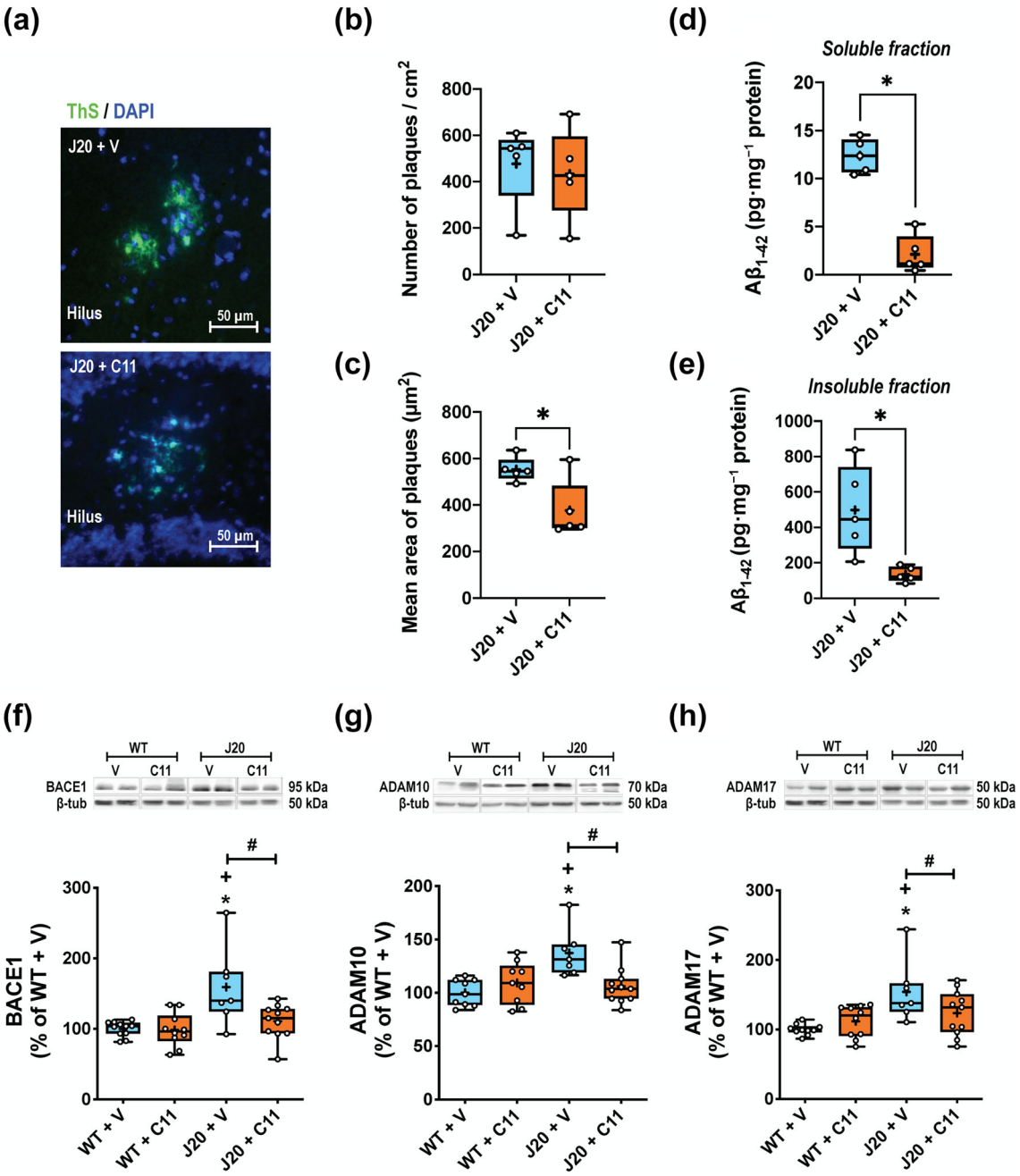

FIGURE 3 Chronic treatment with dazucorilant (C11) blocks Aβ pathology in J20 mice. For experimental protocol see Figure 1a. (a) Brain sections (10 µm) were stained with thioflavin S (ThS, in green) and counterstained with DAPI (in blue) in J20 mice treated with vehicle (J20 + V) or with dazucorilant (J20 + C11). (b,c) Quantification (number) and analysis (size) of amyloid plaques were blindly performed and data are presented as the number of plaques per cm^2 (b) and as the mean area of plaques in μm^2 (c). An unpaired Student's t test was performed. For plaques number: $t = 0.765$ (df = 8), ns; and for plaques sizes: $t = 2.89$ (df = 8), * $P < 0.05$. (d,e) Quantification by ELISA of soluble and insoluble concentrations (*pg/mg protein*) of human $A\beta_{1-42}$ in the hippocampus of J20 mice treated with vehicle (V) or with dazucorilant (C11). An unpaired Student's *t* test was performed. For soluble fraction (d): $t = 8.769$ (df = 8), $P < 0.05$; and for insoluble fraction (e): $t = 3.229$ (df = 8), $P < 0.05$. (f–h) The hippocampal variations of BACE1 (70 kDa, f), ADAM10 (70 kDa, g) and ADAM17 (50 kDa, h) were determined by western blot, normalized with the variations of β-tubulin (β-tub, 55 kDa), and expressed as % of levels obtained in WT mice treated with vehicle (WT + V). A two-way ANOVA followed by a Tukey's multiple comparison were performed. For BACE1: $F_{1,35} = 13.75$ for group ($P < 0.05$); $F_{1,35} = 6.708$ for treatment ($P < 0.05$); and $F_{1,35} = 5.926$ for interaction ($P < 0.05$), for ADAM10: $F_{1,35} = 13.75$ for group ($P < 0.05$); $F_{1,35} = 6.708$ for treatment ($P < 0.05$); and $F_{1,35} = 5.926$ for interaction ($P < 0.05$), and for ADAM17: $F_{1,34} = 12.43$ for group ($P < 0.05$); $F_{1,34} = 1.010$ for treatment (ns); and $F_{1,34} = 5.143$ for interaction ($P < 0.05$). * $P < 0.05$ versus WT + V group. + $P < 0.05$ versus WT + C11 group. # $P < 0.05$ versus selected group. All data are presented as box and whiskers with min to max, median and mean(+) and n = 5-11 mice per group. ns: non-significant.

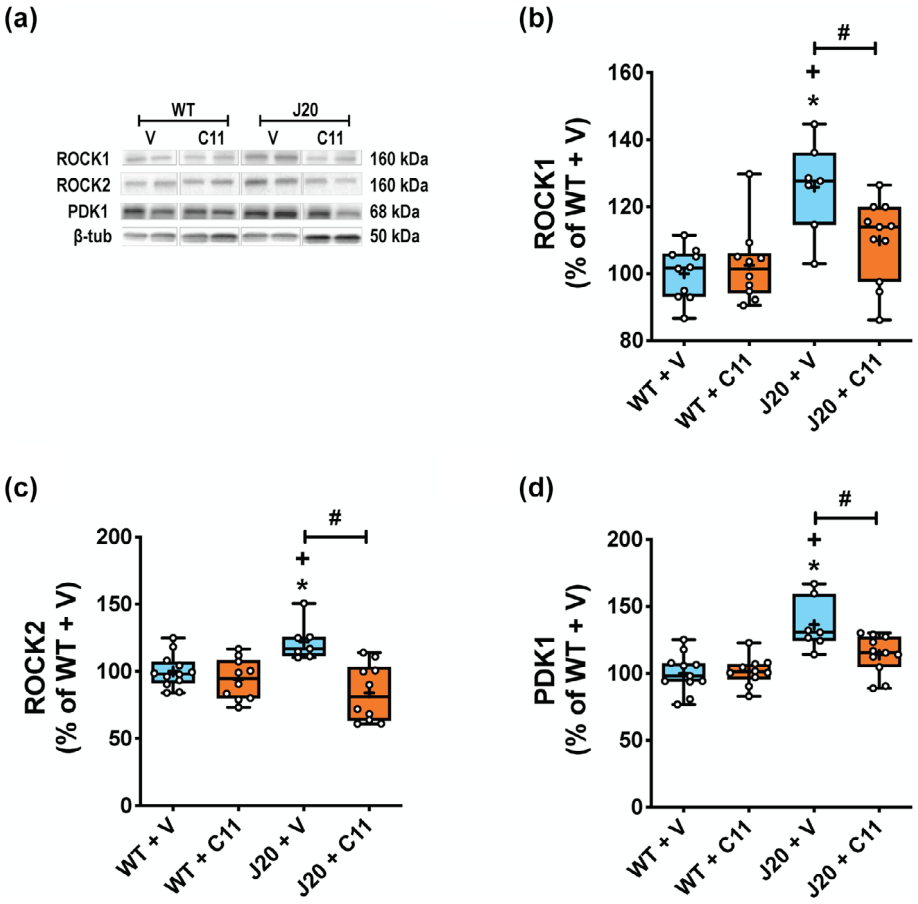

FIGURE 4 Chronic treatment with dazucorilant normalizes ROCK system in J20 mice. For experimental protocol see Figure 1a. Hippocampal variations of ROCK1 (160 kDa, a and b), ROCK2 (160 kDa, a and c) and PDK1 (58–68 kDa, a and c) were determined by western blot, normalized with the variations of β-tubulin (β-tub, 55 kDa) and expressed as % of levels obtained in WT mice treated with vehicle (WT + V). A two-way ANOVA followed by a Tukey's multiple comparison were performed. For ROCK1: $F_{1,34} = 19.9$ for group ($P < 0.05$); $F_{1,34} = 3.30$ for treatment (ns); and $F_{1,34} = 6.26$ for interaction ($P = 0.0173$), for ROCK2: $F_{1,35} = 1.34$ for group (ns); $F_{1,35} = 17.5$ for treatment ($P < 0.05$); and $F_{1,35} = 9.41$ for interaction ($P < 0.05$), and for PDK1: $F_{1,35} = 26.2$ for group ($P < 0.05$); $F_{1,35} = 4.93$ for treatment ($P < 0.05$); and $F_{1,35} = 6.39$ for interaction ($P < 0.05$). * $P < 0.05$ versus WT + V group. + $P < 0.05$ versus WT + C11 group. # $P < 0.05$ versus selected group. All data are presented as box & whiskers with min to max, median and mean(+) and n = 7-12 mice per group. ns: non-significant.

through inhibition of the non-amyloidogenic pathway (Alleaume-Butaux et al., 2015; Henderson et al., 2016). In line with our prior findings in the acute oAβ model of AD (Canet et al., 2020) we observed an upregulation of ROCKs/PDK1 activity in the hippocampus of vehicle-treated J20 mice, which was normalized by dazucorilant administration (Figure 4a,d).

3.5 | Chronic treatment with dazucorilant reverses hippocampal neuroinflammatory processes in J20 mice

Chronic treatment with dazucorilant acts to suppress neuroinflammatory processes in J20 mice. We observed that protein expression of GFAP (a marker of astrocyte activation) (Figure 5a,b) and Iba1 (a marker of microglia recruitment) (Figure 5a,c) were increased in J20 mice, and normalized following dazucorilant treatment. The astrocyte activation and microglia recruitment observed in J20 mice appear to be attributable to an upregulation of protein synthesis, as indicated by the unchanged expression of GFAP mRNA (Figure 5d), and decreased expression levels of triggering receptor expressed on myeloid cells 2 (TREM2; Figure 5e) and hexosaminidase subunit beta (HEXB; Figure 5f) mRNA (two markers of microglial activity). These expression levels were normalized with the dazucorilant treatment (Figure 5e,f). When we evaluated by triple immunohistochemistry the impact of chronic treatment on hippocampal astrocytes (GFAP, Figure 5g), microglia (Iba1, Figure 5h) and amyloid plaques (6E10 labeling), we observed a global reduction of the immunosignal of GFAP and Iba1, and a reduction of plaque size (the latter in line with data from the earlier plaque staining, as previously described; Figure 3). However, it is interesting to note that chronic treatment with dazucorilant induced a redistribution of immune cells towards amyloid plaques (Figure 5g,h). Strikingly, while the signal of astrocytes (GFAP), initially concentrated on amyloid plaques, was decreased (Figure 5g), the microglia signal (Iba1) became particularly intense at the level of amyloid plaques (Figure 5h). Altogether, these findings suggested that dazucorilant might restore the immunosuppressive functions of glucocorticoid receptor in J20 mice.

3.6 | Chronic treatment with dazucorilant reverses the abnormal phosphorylation of tau protein in the hippocampus of J20 mice

We aimed to investigate tau phosphorylation level in J20 mice. Although this model is primarily used for amyloid pathology, we observed a strong hyperphosphorylation of tau protein at several AD-relevant epitopes (i.e. AT180, AT8, AT270 and CP13) (Figure 6a–e), as well as increased levels of TauC3 fragment (tau cleaved at C-term by caspase 3) (Figure 6a,f) in vehicle-treated J20 mice compared to WT controls. Importantly, increased tau phosphorylation at AT180 (T231/

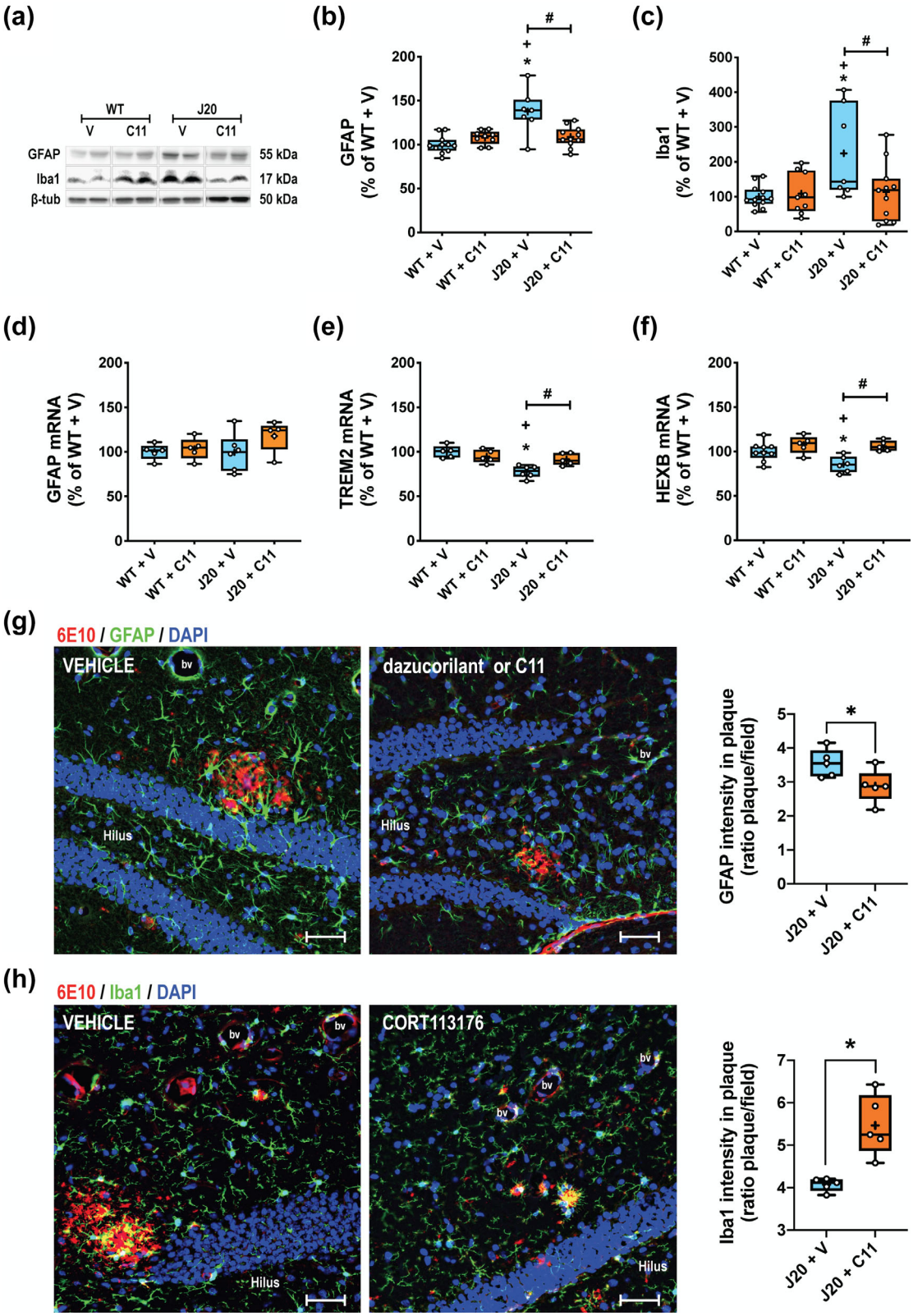

FIGURE 5 Legend on next page.

S235) and cleavage into TauC3 are associated with the inhibition of tau binding to microtubules, and the initiation of tau aggregation in humans (Conze et al., 2022; Sengupta et al., 1998). Moreover, phosphorylation at AT8, AT270 and CP13 is associated with the presence of neurofibrillary tangles (Iqbal et al., 1989; Zheng-Fischhöfer et al., 1998). However, there was no difference in total tau expression or in the phosphorylation level of tau AT100 and PHF1 epitopes between these groups (Figure 6a,g–i). Dazucorilant administration effectively normalized tau phosphorylation at AT180, AT8, AT270 and CP13 (Figure 6a–e), as well as the expression level of TauC3 (Figure 6a,f). The latter result may be explained by a decrease in caspase 3 expression following dazucorilant treatment, as observed in our previous studies (Canet et al., 2020; Pineau et al., 2016).

To elucidate the mechanisms underlying these processes, we assessed the key kinases (**glycogen synthase kinase 3 beta [GSK3B]** and **cyclin dependent kinase 5 [CDK5]**) and phosphatases (PP2A, accounting for 70% of tau dephosphorylation) involved in tau phosphorylation (Martin, Latypova, Wilson, Magnaudeix, Perrin, & Terro, 2013; Martin, Latypova, Wilson, Magnaudeix, Perrin, Yardin, & Terro, 2013). The activity of GSK3B is regulated by phosphorylation at Ser9 and Tyr216. Ser9 phosphorylation inhibits its kinase activity, whereas Tyr216 phosphorylation is required for its full activity (Martin, Latypova, Wilson, Magnaudeix, Perrin, Yardin, & Terro, 2013). Moreover, the activity of **PP2A** is regulated by its methylation at Leu309 at its C-terminus of the catalytic subunit (m-PP2Ac), while its demethylation is indicative of a decreased activity (d-PP2Ac) (Martin, Latypova, Wilson, Magnaudeix, Perrin, & Terro, 2013). At the hippocampal level, vehicle-treated J20 mice exhibited an increase activity of GSK3B, evidenced by elevated phosphorylation at Tyr216 (active form) (Figure 7a,b). Additionally, we observed an increase in CDK5 expression (Figure 7a,d) associated with increased cleavage of p35 into p25 (Figure 7a,e). This activation was accompanied by a significant increase in **Fyn** and **calpain 1** expression (Figure 7a,f,g). Fyn is a Src kinase and calpain 1 is a calcium-activated cystein protease, both involved in AD aetiology and more specifically in GSK3B and CDK5 activation (Jin et al., 2015; Lee et al., 2000; Lesort et al., 1999). Importantly, the activity of the catalytic subunit of PP2A (PP2Ac) was down-regulated, as evidenced by the concomitant increase in demethylation (inactive form) (Figure 7a,h) and decrease in methylation (active form) (Figure 7a,i) (Martin, Latypova, Wilson, Magnaudeix, Perrin, & Terro, 2013). These results collectively suggest that tau hyperphosphorylation in J20 mice may arise from an imbalance between kinase and phosphatase activities. In line with our previous observations in the acute oAβ model of AD (Canet et al., 2020), chronic administration of dazucorilant in J20 mice normalized GSK3B and CDK5 activities (Figure 7a–d), as well as their activators Fyn and Calpain 1 (Figure 7a,f,g). Moreover, the treatment restored the activity of PP2A in J20 mice (Figure 7a,h,i), resulting in the normalization of tau phosphorylation level and cleavage (Figure 7a–f). Finally, dazucorilant, when administered in WT mice, did not induce negative effects on tau phosphorylation or on the expression level of these enzymes.

3.7 | Chronic treatment with dazucorilant reversed AD-related phenotype in 5xFAD mice

In the last set of experiments, we sought to assess the impact of chronic treatment with dazucorilant in a more intense amyloid-producing mouse model, thereby substantiating the therapeutic validity of this compound. We conducted a comparative analysis with J20 mice, focusing on key pathological features for comprehensive insights. 5xFAD mice recapitulate key features of AD pathology from 5 months of age, including Aβ-induced neurodegeneration, senile plaques, neuroinflammation, synaptic and behavioural deficits (Giannoni et al., 2016; Rochais et al., 2020). At 6 months of age, when behavioural deficits and amyloid plaques were prominent (Crouzin et al., 2013), 5xFAD mice (and WT controls) were subjected to the same dazucorilant treatment protocol used for J20 mice (Figure 8a). As observed in J20 mice, dazucorilant treatment in 5xFAD mice restored normal nesting behaviour (Figure 8b) and improved short-

FIGURE 5 Chronic treatment with dazucorilant (C11; CORT113176) re-establishes anti-inflammatory properties of glucocorticoid (GC) in J20 mice. For experimental protocol see Figure 1a. Hippocampal variations of GFAP (50 kDa, a and b) and Iba1 (17 kDa, a and c) were determined by western blot, normalized with the variations of β-tubulin (β-tub, 55 kDa) and expressed as % of levels obtained in WT mice treated with vehicle (WT + V). A two-way ANOVA followed by a Tukey's multiple comparison were performed. For GFAP: $F_{1,34} = 17.1$ for group ($P < 0.05$); $F_{1,34} = 5.13$ for treatment ($P < 0.05$); and $F_{1,34} = 16.03$ for interaction ($P < 0.05$), and for Iba1: $F_{1,35} = 6.43$ for group ($P < 0.05$); $F_{1,35} = 4.06$ for treatment ($P < 0.05$); and $F_{1,35} = 5.58$ for interaction ($P < 0.05$). * $P < 0.05$ versus WT + V group. + $P < 0.05$ versus WT + C11 group. # $P < 0.05$ versus selected group. (d–f) Hippocampal expression of GFAP, TREM2 and hexosaminidase subunit beta (HEXB) mRNA were determined by q-PCR and expressed as% of mRNA levels determined in WT mice treated with the vehicle (WT + V). A two-way ANOVA followed by a Tukey's multiple comparison were performed. For GFAP mRNA: $F_{1,17} = 0.94$ for group (ns); $F_{1,17} = 2.40$ for treatment (ns); and $F_{1,17} = 1.09$ for interaction (ns); for TREM2 mRNA: $F_{1,17} = 17.4$ for group ($P < 0.05$); $F_{1,17} = 2.08$ for treatment (ns); and $F_{1,17} = 9.84$ for interaction ($P < 0.05$); and for HEXB mRNA: $F_{1,21} = 4.25$ for group ($P < 0.05$); $F_{1,21} = 13.3$ for treatment ($P < 0.05$); and $F_{1,21} = 2.685$ for interaction (ns). * $P < 0.05$ versus WT + V group. + $P < 0.05$ versus WT + C11 group. # $P < 0.05$ versus selected group. (g,h) Quantification of GFAP (g) and Iba1 (h) signal intensities (*in green*) at the level of senile plaque (6E10 antibody, in red) was performed by immunohistochemistry in hippocampal sections of J20 mice treated with vehicle (J20 + V) or with dazucorilant (J20 + C11). Brain sections (10 µm) were counterstained with DAPI (in blue) to visualize nuclei and analysis was blindly performed. The GFAP and Iba1 intensities in senile plaques were expressed as the ratio of specific signal in plaques over total respective signal in the totality of the field analysed (cf. *Section 2 for more details*). An unpaired Student's *t* test was performed. For GFAP: $t = 2.327$ ($df = 8$), * $P < 0.05$; and for Iba1: $t = 4.242$ ($df = 8$), * $P < 0.05$. All data are presented as box and whiskers with min to max, median and mean(+) and n = 5-12 mice per group. ns: non-significant.

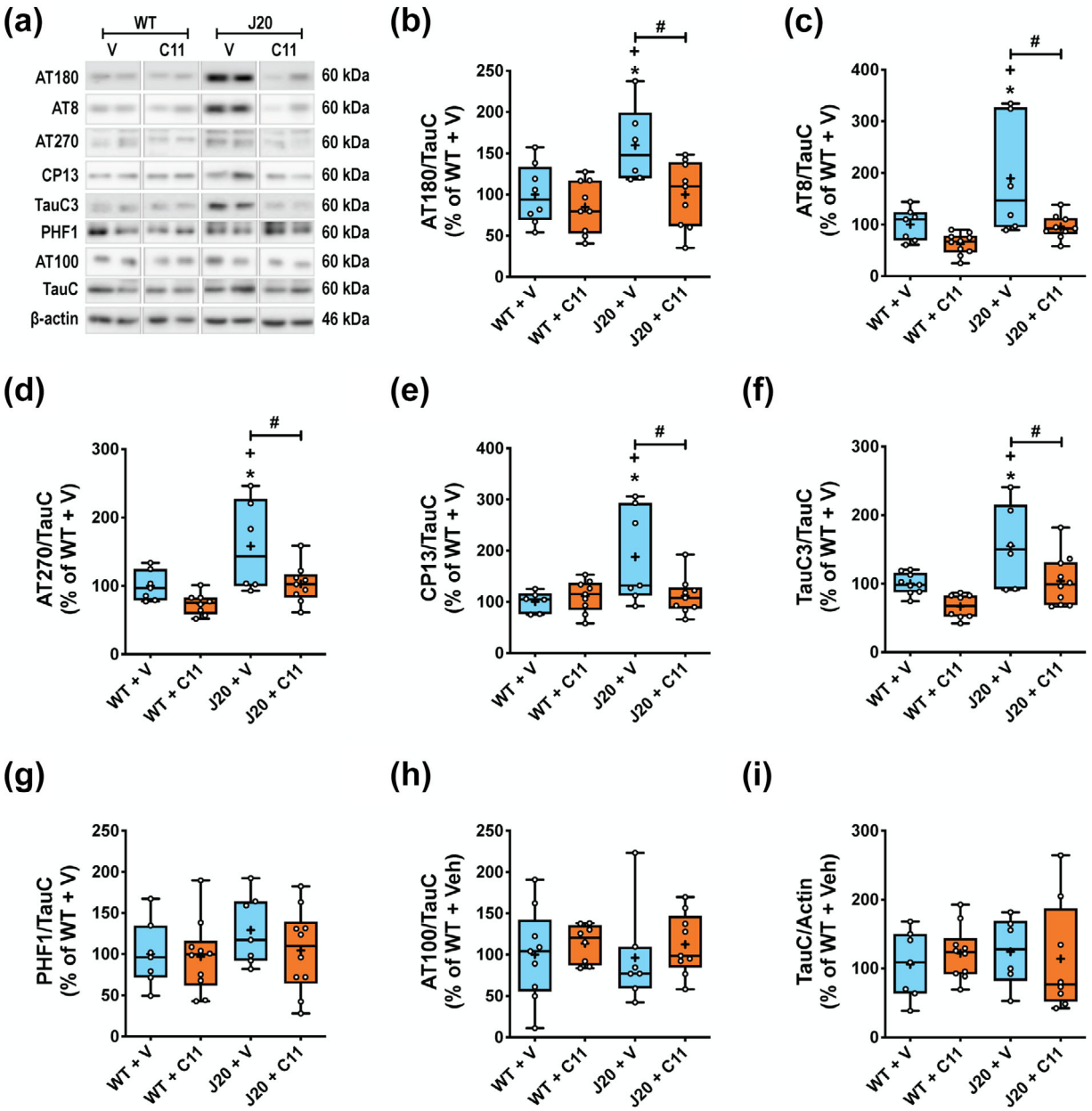

FIGURE 6 Chronic treatment with dazucorilant normalizes phosphorylation levels of tau in J20 mice. For experimental protocol see Figure 1a. Hippocampal variations of tau phosphorylation levels at several AD-relevant epitopes, AT180 (60 kDa), AT8 (60 kDa), AT270 (60 kDa), CP13 (60 kDa), PHF1 (60 kDa), AT100 (60 kDa) and the fragment of tau protein cleaved at C-term by caspase 3 (TauC3, 60 kDa) were determined by western blot, normalized with the variations of tau total (TauC, 60 kDa) or with the variation of actin (46 kDa) in the case of TauC, and expressed as % of levels obtained in WT mice treated with vehicle (WT + V). A two-way ANOVA followed by a Tukey's multiple comparison were performed. For AT180 (a,b): $F_{1,28} = 7.34$ for group ($P < 0.05$); $F_{1,28} = 7.39$ for treatment ($P < 0.05$); and $F_{1,28} = 2.62$ for interaction (ns); for AT8 (a,c): $F_{1,28} = 10.5$ for group ($P < 0.05$); $F_{1,28} = 12.1$ for treatment ($P < 0.05$); and $F_{1,28} = 2.24$ for interaction (ns); for AT270 (a,d): $F_{1,28} = 10.8$ for group ($P < 0.05$); $F_{1,28} = 9.44$ for treatment ($P < 0.05$); and $F_{1,28} = 2.00$ for interaction (ns); for CP13 (a,e); $F_{1,28} = 5.55$ for group ($P < 0.05$); $F_{1,28} = 2.99$ for treatment (ns); and $F_{1,28} = 5.38$ for interaction ($P < 0.05$); for TauC3 (a,f): $F_{1,28} = 14.3$ for group ($P < 0.05$); $F_{1,28} = 11.9$ for treatment ($P < 0.05$); and $F_{1,28} = 0.54$ for interaction (ns); for PHF1 (a,g): $F_{1,28} = 1.35$ for group (ns); $F_{1,28} = 0.8$ for treatment (ns); and $F_{1,28} = 0.49$ for interaction (ns); for AT100 (a,h): $F_{1,28} = 0.02$ for group (ns); $F_{1,28} = 0.85$ for treatment (ns); and $F_{1,28} = 0.007$ for interaction (ns); and for TauC (a,i): $F_{1,28} = 0.06$ for group (ns); $F_{1,28} = 0.02$ for treatment (ns); and $F_{1,28} = 0.42$ for interaction (ns). * $P < 0.05$ versus WT + V group. + $P < 0.05$ versus WT + C11 group. # $P < 0.05$ versus selected group. All data are presented as box and whiskers with min to max, median and mean(+) and n = 6-10 mice per group. ns: non-significant.

and long-term memory performances (Figure 8c,d). Furthermore, the treatment also normalized HPA axis-related parameters, as indicated by the normalization of plasma glucocorticoids levels (Figure 8e), and expression ratios of pglucocorticoid receptor/glucocorticoid receptor (Figure 8f,g) and HSP90/HSP70 (Figure 8f,h). The concomitant re-establishment of plasma corticosterone levels and the expression of

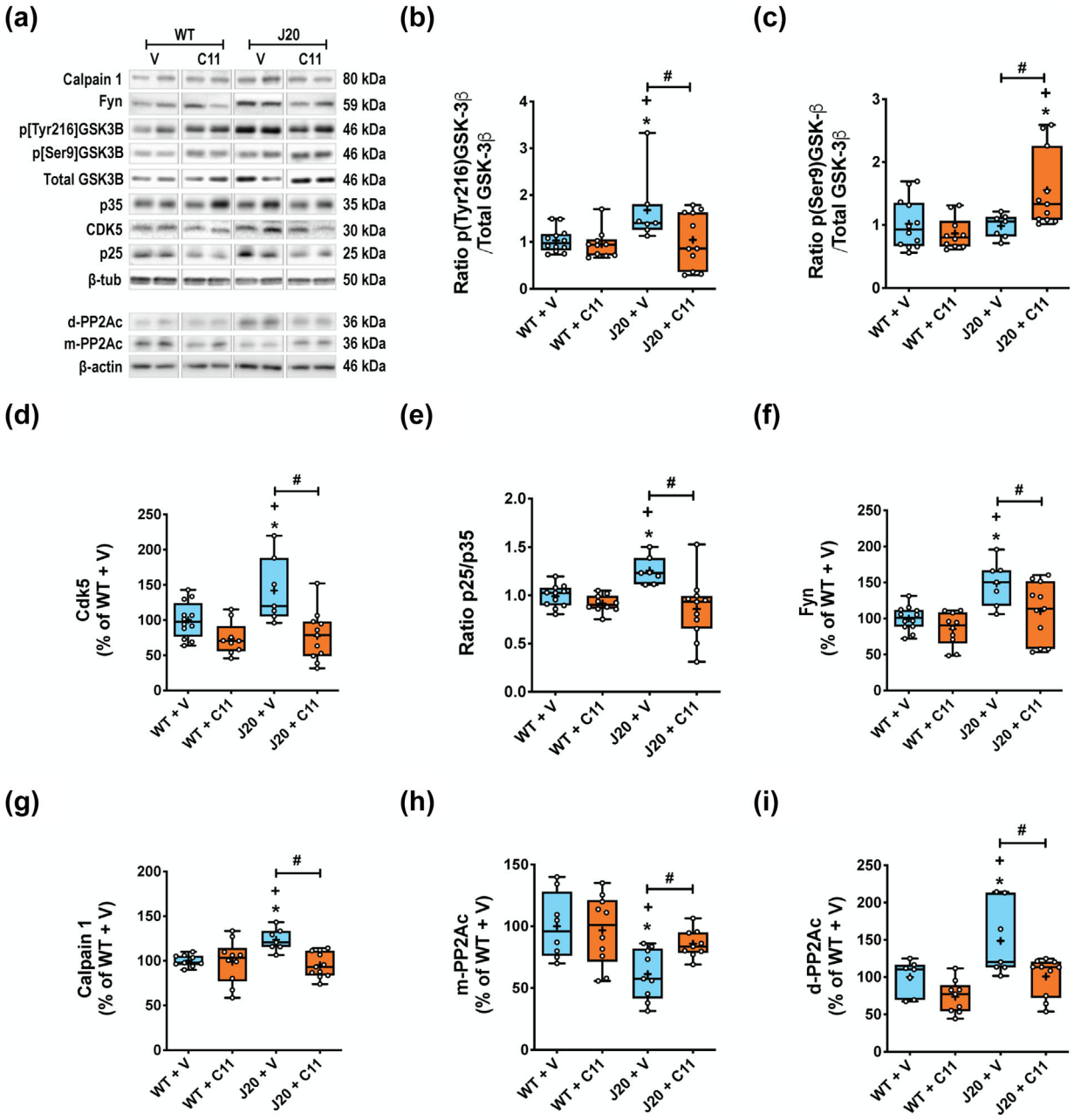

FIGURE 7 Chronic treatment with dazucorilant (C11) normalizes key enzymes involved in the phosphorylation levels of tau in J20 mice. For experimental protocol see Figure 1a. Hippocampal variations of key enzymes involved in tau phosphorylation p (Tyr216) GSK3B(46 kDa), p (Ser9) GSK3B (46 kDa), CDK5 (30 kDa), p25/p35 (25/35 kDa), FYN (59 kDa), Calpain 1 (80 kDa), d-PP2Ac (36 kDa) and m-PP2Ac (36 kDa) were determined by western blot, normalized with the variation of β-tubulin (β-tub, 55 kDa), excepted for the different forms of GSK3B (normalized with total GSK3B variations, 46 kDa), and expressed as % of levels obtained in WT mice treated with vehicle (WT + V). A two-way ANOVA followed by a Tukey's multiple comparison were performed. For p (Tyr216) GSK3B (a,b): $F_{1,36} = 5.52$ for group ($P < 0.05$); $F_{1,36} = 5.16$ for treatment ($P < 0.05$); and $F_{1,36} = 3.16$ for interaction (ns); for p (Ser9) GSK3B (a,c): $F_{1,36} = 5.90$ for group ($P < 0.05$); $F_{1,36} = 2.38$ for treatment (ns); and $F_{1,36} = 7.21$ for interaction ($P < 0.05$); for CDK5 (a,d): $F_{1,36} = 4.55$ for group ($P < 0.05$); $F_{1,36} = 18.2$ for treatment ($P < 0.05$); and $F_{1,36} = 3.23$ for interaction (ns); for p25/p35 (a,e): $F_{1,36} = 2.69$ for group (ns); $F_{1,36} = 13.7$ for treatment ($P < 0.05$); and $F_{1,36} = 6.36$ for interaction ($P < 0.05$); for FYN (a,f): $F_{1,36} = 15.4$ for group ($P < 0.05$); $F_{1,36} = 8.12$ for treatment ($P < 0.05$); and $F_{1,36} = 1.63$ for interaction (ns); for Calpain 1 (a,g): $F_{1,33} = 3.50$ for group (ns); $F_{1,33} = 7.65$ for treatment ($P < 0.05$); and $F_{1,33} = 6.51$ for interaction ($P < 0.05$); for d-PP2Ac (a,h): $F_{1,29} = 12.3$ for group ($P < 0.05$); $F_{1,29} = 11.7$ for treatment ($P < 0.05$); and $F_{1,29} = 0.99$ for interaction (ns); and for m-PP2Ac (a,i): $F_{1,29} = 12.3$ for group ($P < 0.05$); $F_{1,29} = 1.45$ for treatment (ns); and $F_{1,29} = 3.86$ for interaction ($P < 0.05$). * $P < 0.05$ versus WT + V group. + $P < 0.05$ versus WT + C11 group. # $P < 0.05$ versus selected group. All data are presented as box and whiskers with min to max, median and mean(+) and n = 7-12 mice per group. ns: non-significant.

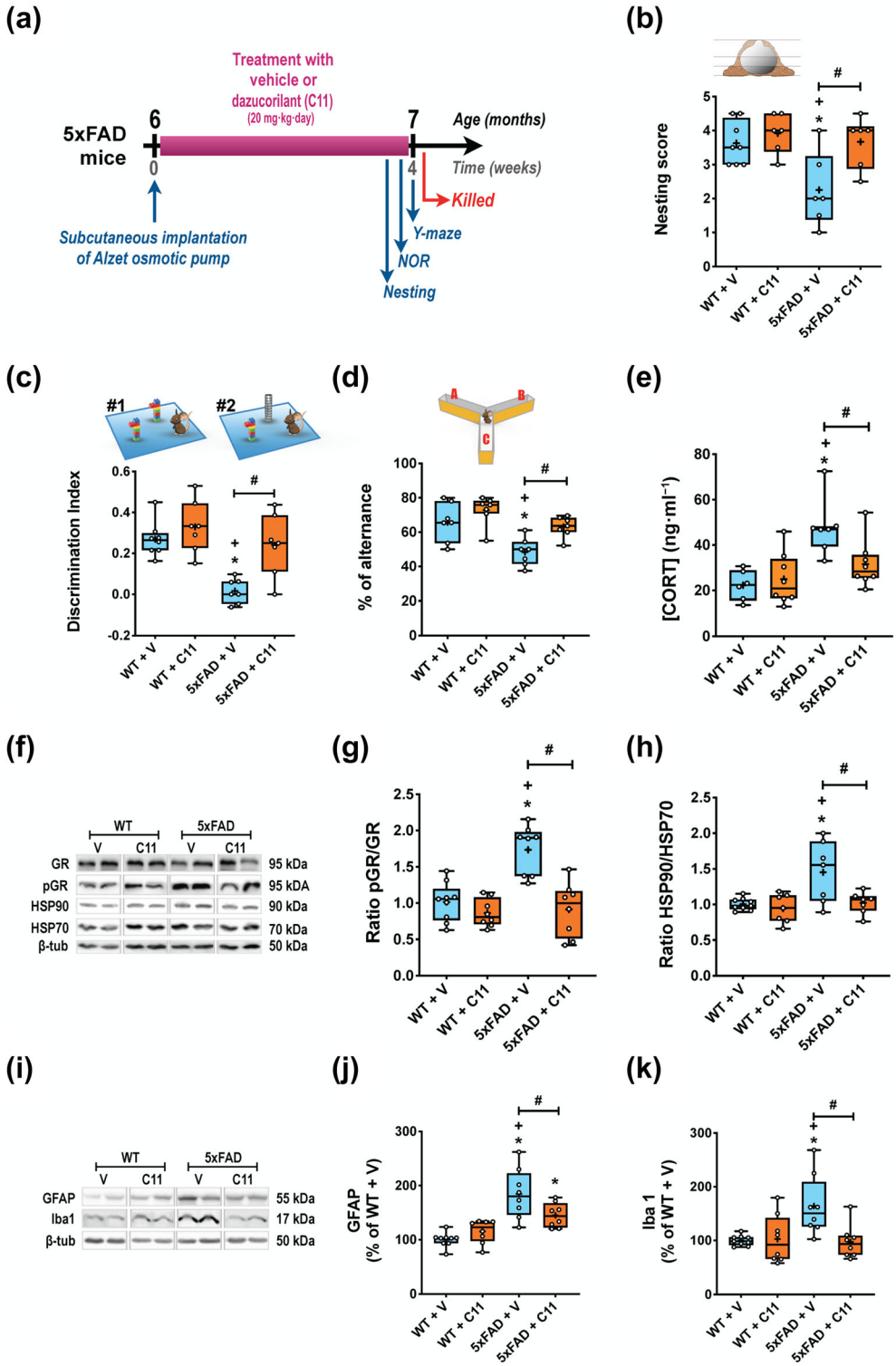

FIGURE 8 Legend on next page.

glucocorticoid receptor-related signalling components by dazucorilant also resulted in an alleviation of neuroinflammation in 5xFAD mice, as evidenced by decreased hippocampal levels of GFAP (Figure 8i,j) and Iba1 (Figure 8i,k). Collectively, these results suggest that dazucorilant effectively inhibits pathways related to glucocorticoid receptor-detrimental overactivation in 5xFAD mice similarly to J20 mice.

Next, we evaluated the ability of dazucorilant to reduce both amyloid and tau pathologies. Notably, dazucorilant administration resulted in a decrease in both soluble and insoluble Aβ_{1-42} fractions (Figure 9a,b), alongside with a downregulation of BACE1 expression (Figure 9c). Dazucorilant treatment also resulted in a reduction of tau phosphorylation at the AT270 epitope (Figure 9d,e) and decreased levels of TauC3 (Figure 9d,f). However, in 6-month-old 5xFAD mice, tau hyperphosphorylation appeared less severe compared to 9-month-old J20 mice, with no observed change in phosphorylation at CP13 or AT180 epitopes, or in total tau levels (Figure 9d–i). Finally, we assessed the same pivotal enzymes involved in tau phosphorylation, revealing that dazucorilant treatment restored normal expression and enzymatic activity of p25, CDK5, GSK3B, Fyn, calpain 1 and PP2A, all of which were impaired in 5xFAD mice (Figure 10a–h). Altogether, our data validated the efficacy of dazucorilant at counteracting neurodegenerative pathways in 5xFAD mice, supporting its viability as a therapeutic compound for AD.

4 | DISCUSSION

Detrimental and pathological glucocorticoid receptor overactivation plays a pivotal role in AD pathophysiology, connecting amyloid and tau pathologies (Baglietto-Vargas et al., 2013; Canet et al., 2018; Canet et al., 2020). Dazucorilant belongs to a novel class of selective non-steroidal glucocorticoid receptor ligands with excellent affinity for the glucocorticoid receptor (Beaudry et al., 2014; Pineau et al., 2016). The term selective glucocorticoid receptor modulator (sGRm) reflects its biological properties, as dazucorilant exhibits partial antagonism and some agonism in a transrepression assay (Gazorpak et al., 2023; Pineau et al., 2016), enabling selective abrogation of glucocorticoid receptor-dependent pathogenic processes in the brain, while potentially retaining the beneficial aspects of glucocorticoid receptor signalling (Meijer et al., 2018; Pineau et al., 2016). While previous studies from our group reported its ability to effectively reverse oAβ-induced pathology (Canet et al., 2020; Pineau et al., 2016), we here demonstrate for the first time the therapeutic potential of dazucorilant in two transgenic AD models, that is the J20 and 5xFAD mouse lines. Our results evidence that a 4-week chronic administration of dazucorilant (i), restored the physiological levels of circulating corticosterone, (ii) the neuronal expression, phosphorylation and localization of glucocorticoid receptor, (iii) reversed neuroinflammatory processes and reduced amyloid and tau pathologies, along with (iv) improved memory performance. Notably, treatment with dazucorilant did not induce any adverse effects on all evaluated parameters, in WT, J20 or 5xFAD mice.

Chronic administration of dazucorilant to J20 and 5xFAD mice inhibited amyloidogenic pathways concurrently with the normalization of circulating glucocorticoids levels and reversal of changes in glucocorticoid receptor-related signalling pathways. These observations include normalization of glucocorticoid receptor phosphorylation status and cellular localization, as well as expression of glucocorticoid receptor chaperones HPS90/HSP70 and the glucocorticoids-converting enzyme 11-βHSD1, and kinases linked to glucocorticoid

FIGURE 8 Chronic treatment with dazucorilant prevents behavioural impairments, normalizes glucocorticoid receptor (GR) activity and re-establishes the anti-inflammatory properties of glucocorticoids (GC) in 5xFAD mice. (a) Experimental protocol at T0, at the age of 6 months, 5xFAD mice and wildtype (WT) littermates were subcutaneously implanted with an osmotic micropump (Alzet®) that delivered during 4 weeks 20 mg·kg^{-1}·day^{-1} of dazucorilant (C11), or a vehicle solution (V). At the age of 7 months, behavioural performances of all mice were tested. (b) Overall welfare behaviour was determined by the nesting test. Nest building was scored according to a described rating scale of 1–5 (Hess et al., 2008). A two-way ANOVA followed by a Tukey's multiple comparison were performed: $F_{1,22} = 6.99$ for group ($P < 0.05$); $F_{1,22} = 7.73$ for treatment ($P < 0.05$); and $F_{1,22} = 3.35$ for interaction ns. (c) Recognition memory was determined using the novel object recognition (NOR) test. The recognition memory sensitivity was evaluated by calculating the preferential discrimination index (Sivakumaran et al., 2018). A two-way ANOVA followed by a Tukey's multiple comparison were performed: $F_{1,25} = 17.4$ for group ($P < 0.05$); $F_{1,25} = 12.0$ for treatment ($P < 0.05$); and $F_{1,25} = 3.97$ for interaction ($P < 0.05$). (d) Spontaneous working memory performance was determined in a Y maze test. The number of arm entries and the number of triads were recorded to calculate the percentage of alternations. A two-way ANOVA followed by a Tukey's multiple comparison were performed: $F_{1,24} = 17.3$ for group ($P < 0.05$); $F_{1,24} = 11.2$ for treatment ($P < 0.05$); and $F_{1,24} = 1.40$ for interaction (ns). (e) Plasma concentrations of corticosterone (CORT) were determined by ELISA and expressed as ng·ml^{-1}. Two-way ANOVA: $F_{1,25} = 16.5$ for group ($P < 0.05$); $F_{1,25} = 2.93$ for treatment (ns); and $F_{1,25} = 5.68$ for interaction ($P < 0.05$). Hippocampal variations of GR (95 kDa), its phosphorylation level (p [Ser211]GR, 95 kDA), HSP90 and HSP70 levels (90 kDa and 70 kDa, respectively) were determined by western blot, normalized with the variations of β-tubulin (β-tub, 55 kDa) and expressed as the ratio of pGR/GR (f and g) and HSP90/HSP70 (f and h). A two-way ANOVA followed by a Tukey's multiple comparison were performed. For pGR/GR: $F_{1,29} = 13.7$ for group ($P < 0.05$); $F_{1,29} = 21.8$ for treatment ($P < 0.05$); and $F_{1,29} = 10.4$ for interaction ($P < 0.05$); and for HSP90/HSP70: $F_{1,26} = 8.67$ for group ($P < 0.05$); $F_{1,26} = 7.45$ for treatment ($P < 0.05$); and $F_{1,26} = 4.24$ for interaction ($P < 0.05$). Hippocampal variations of GFAP (50 kDa, i and j) and Iba1 (17 kDa, i and k) were determined by western blot, normalized with the variations of β-tubulin (β-tub, 55 kDa) and expressed as % of levels obtained in WT mice treated with vehicle (WT + V). A two-way ANOVA followed by a Tukey's multiple comparison were performed. For GFAP: $F_{1,29} = 33.9$ for group ($P < 0.05$); $F_{1,29} = 1.52$ for treatment (ns); and $F_{1,34} = 7.83$ for interaction ($P < 0.05$), and for Iba1: $F_{1,25} = 6.46$ for group ($P < 0.05$); $F_{1,25} = 6.656$ for treatment ($P < 0.05$); and $F_{1,25} = 4.17$ for interaction ($P < 0.05$). * $P < 0.05$ versus WT + V group. + $P < 0.05$ versus WT + C11 group. # $P < 0.05$ versus selected group. All data are presented as box and whiskers with min to max, median and mean(+) and n = 6-9 mice per group. ns: non-significant.

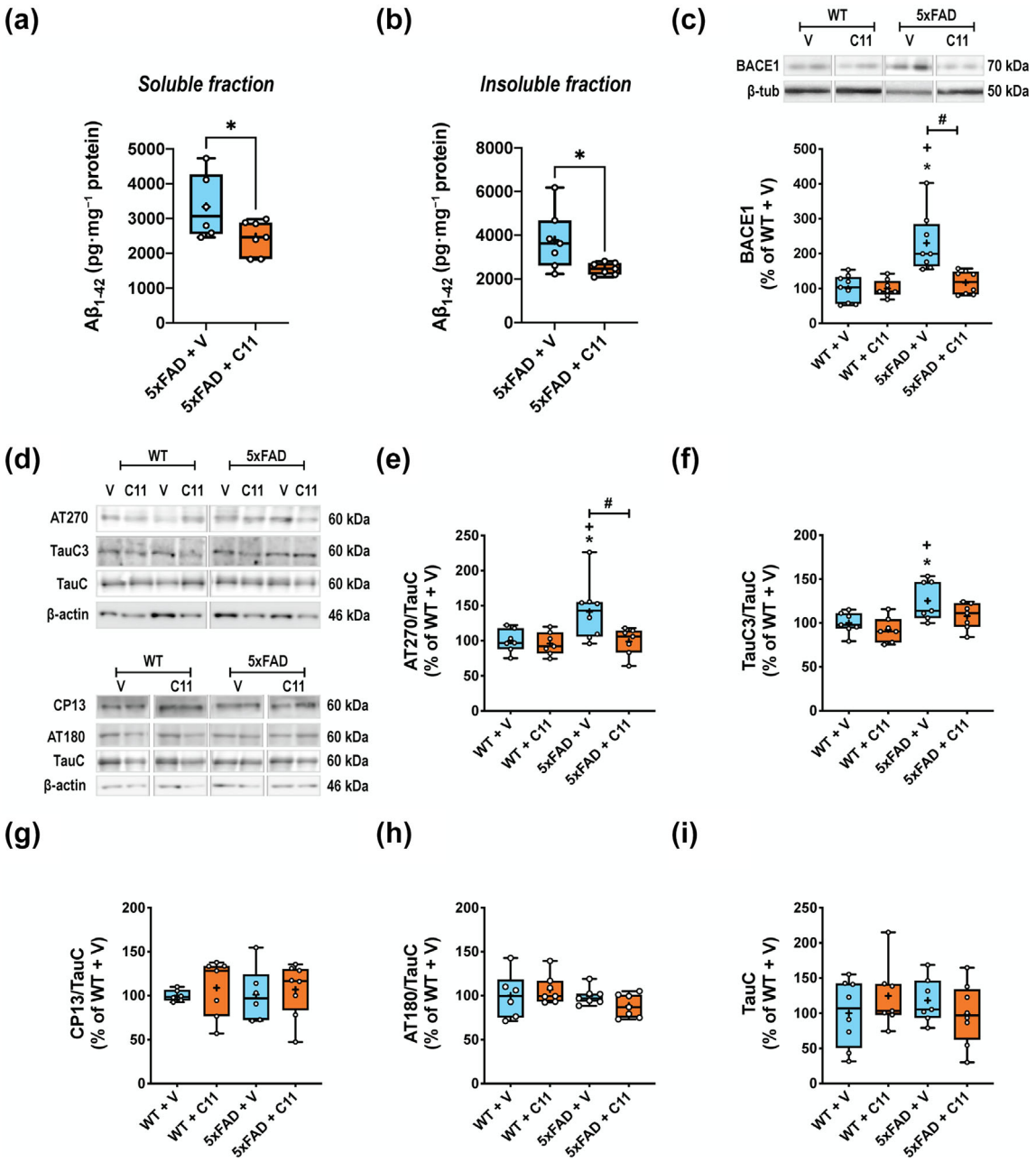

FIGURE 9 Chronic treatment with dazucorilant (C11) blocks Aβ pathology and normalizes phosphorylation levels of tau in 5xFAD mice. For experimental protocol see Figure 8a. (a,b) Quantification by ELISA of soluble and insoluble concentrations (pg·mg^{-1} protein) of human Aβ_{1-42} in the hippocampus of 5xFAD mice treated with vehicle (V) or with dazucorilant (C11). An unpaired Student's t test was performed. For soluble fraction (a): $t = 2.211$ (df = 11), $P < 0.05$; and for insoluble fraction (B): $t = 2.504$ (df = 12), $P < 0.05$. * $P < 0.05$ versus 5xFAD + V group. (c) Hippocampal variations of BACE1 (70 kDa) were determined by western blot, normalized with the variations of β-tubulin (β-tub, 55 kDa) and expressed as % of levels obtained in WT mice treated with vehicle (WT + V). A two-way ANOVA followed by a Tukey's multiple comparison were performed: $F_{1,29} = 17.4$ for group ($P < 0.05$); $F_{1,29} = 10.4$ for treatment ($P < 0.05$); and $F_{1,29} = 10.4$ for interaction ($P < 0.05$). (d–i) Hippocampal variations of tau phosphorylation level at several AD-relevant epitopes AT270 (60 kDa), CP13 (60 kDa), AT180 (60 kDa) and the fragment of tau protein cleaved AT C-term by caspase-3 (TauC3, 60 kDa) were determined by western blot, normalized with the variations of total tau (TauC, 60 kDa) or with the variation of actin (46 kDa) in the case of TauC, and expressed as % of levels obtained in WT mice treated with vehicle (WT + V). A two-way ANOVA followed by a Tukey's multiple comparison were performed. For AT270 (d and e): $F_{1,24} = 5.62$ for group ($P < 0.05$); $F_{1,24} = 4.47$ for treatment ($P < 0.05$); and $F_{1,24} = 4.36$ for interaction ($P < 0.05$); for TauC3 (d and f): $F_{1,24} = 10.5$ for group ($P < 0.05$); $F_{1,24} = 4.00$ for treatment ($P < 0.05$); and $F_{1,24} = 0.66$ for interaction (ns); for CP13 (d and g): $F_{1,23} = 0.002$ for group (ns); $F_{1,23} = 0.45$ for treatment (ns); and $F_{1,23} = 0.02$ for interaction (ns); for AT180 (d and h): $F_{1,23} = 2.08$ for group (ns); $F_{1,23} = 0.08$ for treatment (ns); and $F_{1,23} = 1.82$ for interaction (ns); and for TauC (d and i): $F_{1,24} = 0.06$ for group (ns); $F_{1,24} = 0.03$ for treatment (ns); and $F_{1,24} = 1.95$ for interaction (ns). * $P < 0.05$ versus WT + V group. + $P < 0.05$ versus WT + C11 group. # $P < 0.05$ versus selected group. All data are presented as box and whiskers with min to max, median and mean(+) and n = 6-9 mice per group. ns: non-significant.

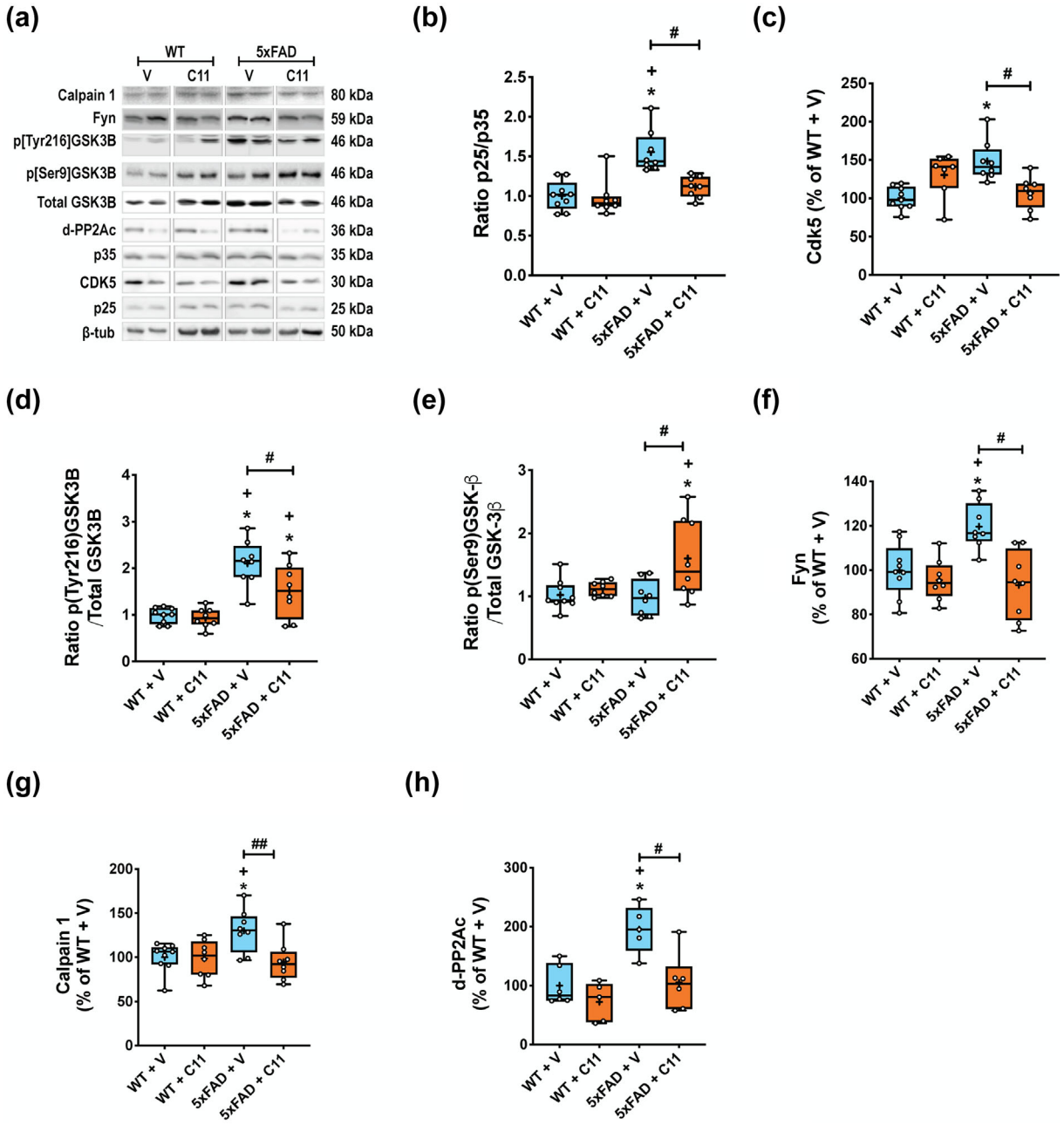

FIGURE 10 Chronic treatment with dazucorilant (C11) normalizes key enzymes involved in the phosphorylation levels of tau in 5xFAD mice. For experimental protocol see Figure 8a. Hippocampal variations of key enzymes involved in tau phosphorylation—p25/p35 (25/35 kDa), CDK5 (30 kDa), p (Ser9) GSK3B (46 kDa), p (Tyr216) GSK3B (46 kDa), Fyn (59 kDa), calpain 1 (80 kDa) and d-PP2Ac (36 kDa) were determined by western blot, normalized with the variation of β-tubulin (β-tub, 55 kDa), excepted for the different forms of GSK3B (normalized with total GSK3B variations, 46 kDa) and expressed as % of levels obtained in WT mice treated with vehicle (WT + V). A two-way ANOVA followed by a Tukey's multiple comparison were performed. For p25/p35 (a,b): $F_{1,25} = 20.9$ for group ($P < 0.05$); $F_{1,25} = 6{,}60$ for treatment ($P < 0.05$); and $F_{1,25} = 3.00$ for interaction (ns); for CDK5 (a,c): $F_{1,29} = 1.29$ for group (ns); $F_{1,29} = 0.12$ for treatment (ns); and $F_{1,29} = 21.7$ for interaction ($P < 0.05$); for p (Ser9) GSK3B(a,d): $F_{1,29} = 2.98$ for group (ns); $F_{1,29} = 6.87$ for treatment ($P < 0.05$); and $F_{1,29} = 4.24$ for interaction ($P < 0.05$); p (Tyr216)GSK3B (a,e): $F_{1,29} = 37.7$ for group ($P < 0.05$); $F_{1,29} = 5.38$ for treatment ($P < 0.05$); and $F_{1,36} = 3.86$ for interaction ($P < 0.05$); for Fyn (a,f): $F_{1,29} = 4.31$ for group ($P < 0.05$); $F_{1,29} = 13.7$ for treatment ($P < 0.05$); and $F_{1,29} = 6.94$ for interaction ($P < 0.05$); for calpain 1 (a,g): $F_{1,29} = 3.27$ for group (ns); $F_{1,29} = 6.52$ for treatment ($P < 0.05$); and $F_{1,29} = 5.50$ for interaction ($P < 0.05$); and for d-PP2Ac (a and h): $F_{1,18} = 14.2$ for group ($P < 0.05$); $F_{1,18} = 12.1$ for treatment ($P < 0.05$); and $F_{1,18} = 3.46$ for interaction (ns). * $P < 0.05$ versus WT + V group. + $P < 0.05$ versus WT + C11 group. # $P < 0.05$ versus selected group. All data are presented as box & whiskers with min to max, median and mean(+) and n = 5-9 mice per group. ns: non-significant.

receptor activity. We cannot conclude that there was overall glucocorticoid receptor overactivation in J20 mice, given that FKBP5 mRNA was unchanged. Yet, a degree of glucocorticoid receptor overactivation is further supported by the nuclear accumulation of glucocorticoid receptor in CA1 hippocampal neurons observed in J20 mice. These observations were made with epifluorescent microscopy and would need further investigation to determine the precise subcellular localization of glucocorticoid receptor. However, this is consistent with our previous findings in the acute oAβ model of AD (Brureau et al., 2013) and with the observed disruption of glucocorticoid negative feedback in AD patients (Csernansky et al., 2006; Hartmann et al., 1997; Hoogendijk et al., 2006). Additionally, there was a clear elevation of ANXA1, a potent endogenous anti-inflammatory effector released by CNS immune and endothelial cells upon glucocorticoid receptor phosphorylation and activation by glucocorticoids (Perretti & D'Acquisto, 2009; Sugimoto et al., 2016).

The suppression of APP and BACE1 protein expression after dazucorilant likely results from antagonism of the direct genomic action of glucocorticoid receptor on the glucocorticoid-responsive elements (GRE) within their respective genes (Lahiri, 2004; Sambamurti et al., 2004). These results might also explain the observed reduction in soluble Aβ1–42 levels and amyloid plaques size. Furthermore, recent evidence has indicated that glucocorticoids can facilitate the interaction between APP and BACE1 (Zhuravleva et al., 2021), implying that dazucorilant may not only affect the expression of APP and BACE1, but also prevent their interaction. Additionally, dazucorilant treatment concurrently promoted the non-amyloidogenic pathway by downregulating the ROCK/PDK1 system, as previously observed (Canet et al., 2020). Glucocorticoid receptor can directly activate these kinases involved in crucial cellular functions (cell motility, cell proliferation, autophagy and apoptosis) (Rubenstein et al., 2007). Notably, ROCK/PDK1 activity is exacerbated in AD, inhibiting soluble amyloid precursor protein alpha (sAPPα) formation and thus promoting the amyloidogenic pathway (Alleaume-Butaux et al., 2015). These findings position ROCK/PDK1 as promising therapeutic targets in AD, especially since ROCKs depletion has been shown to directly decrease Aβ levels (Henderson et al., 2016). Our observations indicate that dazucorilant counteracts ROCK/PDK1 overactivation in J20 mice, which coincided with reduced levels of soluble and insoluble Aβ_{1-42} in the hippocampus. Moreover, data from J20 mice showed that 4 weeks treatment reduced amyloid plaque size without significantly affecting plaque number. Although this reduction may primarily reflect a direct suppression of Aβ peptide synthesis, we cannot exclude that treatment also promotes the expression of enzymes such as **IDE (insulin degrading enzyme)** responsible for amyloid degradation, as we have previously reported (Canet et al., 2020).

The regulation of neuroinflammatory processes in AD remains a complex and critical area of research. Glucocorticoids are pivotal negative modulators of immune responses in the periphery and CNS (Canet et al., 2019; Fonken et al., 2018; Leng & Edison, 2021). However, in the brain, glucocorticoids can also exert proinflammatory effects through the potentiation of NRLP3 inflammasome, contributing to the pathogenesis of several inflammatory disorders, potentially including AD (Canet et al., 2019; Fonken et al., 2018; Leng & Edison, 2021). In support, we recently found that chronic glucocorticoid consumption before the induction of Aβ pathology exacerbates both pro-inflammatory processes and AD-related symptoms, indicating ineffective glucocorticoid-mediated immunosuppression in an AD context (Canet et al., 2022). J20 and 5xFAD mice exhibited heightened neuroinflammation concurrent with elevated glucocorticoid levels. The increased hippocampal ANXA1 mRNA levels in J20 mice did not coincide with an effective anti-inflammatory activity, aligning with the increased expression of ANXA1 observed in AD patients brains (Ries et al., 2016), and while glucocorticoid receptor induction of ANAX1 is intact this does not suffice to ameliorate the disease process in AD. In fact, dazucorilant treatment mitigated neuroinflammatory processes by impeding the glucocorticoid receptor pathological overactivity. Notably, dazucorilant seems to refine the immune response specificity in J20 mice. Post-treatment, a withdrawal of astrocytes from amyloid plaques was observed, enabling focused microglial engagement and contributing to plaque size reduction. Interestingly, a similar effect has been documented in 5xFAD mice having received a TREM2-activating antibody, which promotes microglia clustering around amyloid plaques, thereby improving cognition (Price et al., 2020). TREM2 is essential for promoting microglial association with amyloid plaques and proliferation around them (Hansen et al., 2018; Jay et al., 2015; Wang et al., 2016). Studies have also shown that astrocytes and microglia compete to clear amyloid deposits, with astrocytes being less efficient (Söllvander et al., 2016). Moreover, there is a crosstalk between reactive astrocytes and microglia, where each cell type can inhibit the phagocytic capacity of the other (DeWitt et al., 1998; Liddelow et al., 2017). Treatment with dazucorilant not only reduced astrocyte reactivity and their presence around plaques, but also restored TREM2 mRNA levels. These effects coincided with an increased presence of microglial cells surrounding plaques and a reduction in amyloid burden and plaque size, strongly suggesting that dazucorilant promotes microglial phagocytosis by mitigating astrocyte reactivity. While further additional analyses are warranted to fully support these interpretations, our data posit dazucorilant as a potent immunomodulator, aligning with previous reports in others neurodegenerative disorders (De Nicola et al., 2020; Gentenaar et al., 2024).

J20 and 5xFAD mice are commonly used models to study amyloid pathology, but they also exhibit hyperphosphorylated tau, supporting the amyloid cascade hypothesis. Specifically, tau hyperphosphorylation occurred at AD-relevant epitopes and included the abnormal caspase 3-mediated tau cleavage into TauC3 fragment (Conze et al., 2022; Iqbal et al., 1989; Sengupta et al., 1998), which dazucorilant treatment inhibited. Elevated TauC3 expression, highly pathogenic due to its propagation and seeding properties, is found in CSF of patients (Borroni et al., 2009; Conze et al., 2022; Plouffe et al., 2012). Tau phosphorylation is primarily regulated by GSK3B and CDK5 (Martin, Latypova, Wilson, Magnaudeix, Perrin, Yardin, & Terro, 2013), and dephosphorylation by PP2A (Martin, Latypova, Wilson, Magnaudeix, Perrin, & Terro, 2013). Our study reports aberrant enzyme activities in J20 and 5xFAD mice, with GSK3B and CDK5

overactivation as evidenced by increased Tyr216 phosphorylation and enhanced cleavage of p35 to p25, respectively. Notably, CDK5 may also contribute to amyloid production by stimulating BACE1 (Quan et al., 2019). Conversely, PP2A activation via methylation at Leu309 was significantly decreased, possibly contributing to tau hyperphosphorylation. We have recently positioned glucocorticoids as central regulators of tau phosphorylation processes (Canet et al., 2020), as they modulate GSK3B, CDK5 and PP2A activities either by direct non-genomic, or indirect mechanisms (Dey et al., 2017; Paliogianni et al., 1995; Panettieri et al., 2019). Moreover, PP2A deficiency affects glucocorticoid receptor nuclear trafficking and glucocorticoid sensitivity (Kobayashi et al., 2011), which may contribute to neuroinflammation in J20 mice, despite increased levels of glucocorticoids. In both models, dazucorilant treatment normalized GSK3B, CDK5 and PP2A activities, resulting in tau dephosphorylation, emphasizing the complex glucocorticoid receptor-enzymes interplay to regulate tau phosphorylation. Moreover, ROCK/PDK1 activation may also participate in tau hyperphosphorylation through GSK3B and CDK5 activation (Castro-Alvarez et al., 2011; Hamano et al., 2012). This further underscores the importance of attenuating glucocorticoid-mediated ROCK/PDK1 activation to lower tau phosphorylation, as reported (Castro-Alvarez et al., 2011). Our findings provide new insights into how reestablishing glucocorticoid receptor function can directly lower tau hyperphosphorylation by rebalancing key enzymes activities.

We also emphasize the significance of other enzymes contributing to tau hyperphosphorylation that are directly regulated by the activity of glucocorticoid receptors. Fyn, for instance, acts as a chaperone for inactive glucocorticoid receptors and is released upon glucocorticoid binding, mediating the rapid non-genomic effects of these receptors (Petta et al., 2016). Under physiological conditions, glucocorticoids play an inhibitory role on Fyn (Löwenberg et al., 2005), while chronic stress and elevated glucocorticoid levels exacerbate their activity (Li et al., 2007). Fyn has been demonstrated to rapidly induce tau phosphorylation either directly on tyrosine residues (Martin, Latypova, Wilson, Magnaudeix, Perrin, Yardin, & Terro, 2013; Scales et al., 2011) or via the activation of GSK3B (Lesort et al., 1999). These findings are consistent with our current observations showing a concomitant increase in Fyn and GSK3B expressions and tau hyperphosphorylation in J20 and 5xFAD mice. Finally, Fyn has been implicated in mediating the activation of the ROCK/PDK1 system (Lv et al., 2016), suggesting an indirect impact on amyloid production. Additionally, the cysteine protease calpain 1 is a well-known enzyme involved in the pathophysiology of AD (Jin et al., 2015) and appears to be up-regulated in both J20 and 5xFAD mice. Calpain 1 has been shown to disrupt p25/CDK5 activity and promote its intracellular accumulation, thereby mediating tau hyperphosphorylation and apoptosis (Lee et al., 2000). Importantly, it has been demonstrated that glucocorticoids can trigger the activation of calpain 1 via an unidentified mechanism (Liu et al., 2012). While a glucocorticoid-responsive elements has been identified in the **calpain 2** gene (*Capn2*) sequence (Hong & Forsberg, 1995), it has not been found in the calpain 1 gene (*Capn1*) so far. Finally, dazucorilant treatment leads to the normalization of Fyn and calpain 1 expression, thereby contributing to the mitigation of amyloid production and tau phosphorylation. In summary, these findings underscore the importance of impeding glucocorticoid receptor-dependent pathogenic processes to regulate the activities of a multitude of enzymes.

We present a schematic representation illustrating the central role of glucocorticoid receptor in the pathophysiological regulation of the pathways described below (see graphic abstract). However, it is important to conduct further investigations to gain a deeper understanding of the molecular mechanisms underlying these regulations. In our current state of knowledge, glucocorticoid receptor are nuclear receptors that regulate gene expression in three main ways:- (i) directly, by binding to glucocorticoid response elements (GRE), (ii) indirectly, through the modulation of specific transcription factors or (iii), via non-genomic mechanisms, which encompass epigenetic modifications, membrane localization and/or heterodimerization with other receptors (reviewed in Groeneweg et al., 2011; Panettieri et al., 2019; Timmermans et al., 2019). Notably, amyloid toxicity may promote the binding of glucocorticoids to the putative membrane glucocorticoid receptor (Choi et al., 2017) which mediate part of the non-genomic glucocorticoid effects. Activation of these receptors has been linked to enhanced glutamatergic transmission and calcium excitotoxicity (Groeneweg et al., 2011), as well as the stimulation of GSK3B (Jozic et al., 2017) and BACE1 (Choi et al., 2017). These findings introduce additional intracellular pathways by which glucocorticoid receptor may exacerbate AD pathophysiology. Based on our prior research (Canet et al., 2020; Pineau et al., 2016) and the current results obtained, we can speculate that some of the beneficial effects of selective glucocorticoid receptor modulators may not be solely attributed to the inhibition of glucocorticoid receptor pathological transcriptional activity but also involve restoring the non-genomic actions of these receptors. However, direct non-genomic effects have not been evaluated for dazucorilant. Further investigations are needed to elucidate the precise contribution of membrane glucocorticoid receptor compared to cytoplasmic/nuclear glucocorticoid receptor. These findings underline the potential significance of developing drugs targeting membrane glucocorticoid receptor, thereby regulating only a subset of glucocorticoid receptor-associated pathways.

Several clinical trials involving selective glucocorticoid receptor modulators are currently underway. As previously discussed, the term 'selective glucocorticoid receptor modulators (sGRm)' denotes the specific biological properties of this group of molecules. More precisely, when these compounds bind to glucocorticoid receptor they induce a distinct pattern of nuclear coregulator recruitment resulting in a unique profile of genomic regulations (Sundahl et al., 2015; Viho et al., 2019). These distinctive features enable these molecules to potentially selectively inhibit glucocorticoid receptor-dependent pathogenic processes in the brain as antagonists, while preserving beneficial aspects of glucocorticoid receptor signalling as agonists (for comprehensive details, see Meijer et al., 2018; Pineau et al., 2016; Sundahl et al., 2015; Viho et al., 2019). The selective glucocorticoid receptor modulator family has generated considerable interest due to its ability to enable the physiological functioning of glucocorticoid receptor, in contrast to conventional antagonists such as

mifepristone. We have evidenced that mifepristone shows less efficacy than selective glucocorticoid receptor modulators in improving AD-related pathology in the acute oAβ model (Pineau et al., 2016). It is also noteworthy that the administration of mifepristone was tested in AD patients but was abandoned (Belanoff et al., 2002). According to information available on the clinical trial listings on https://www.clinicaltrials.gov/, four selective glucocorticoid receptor modulators are currently undergoing clinical testing for conditions associated with glucocorticoid dysregulation, each exhibiting varying degrees of affinity for glucocorticoid receptor. Specifically, **mapracorat (ZK-245186**; Intendis/Bayer) is an FDA-approved drug for treating atopic dermatitis. Additionally, among Corcept Therapeutics molecules, relacorilant (CORT125134) in phase III trials for ovarian cancer and Cushing's syndrome. It is also being evaluated in prostate cancer in combination with the **androgen receptor (NR3C4)** antagonist, **enzalutamide**. **Miricorilant (CORT118335**) is being evaluated in patients with non-alcoholic fatty liver disease. Finally, the compound of interest in this study, dazucorilant is in a phase II clinical trial for treating amyotrophic lateral sclerosis and has demonstrated encouraging results in preclinical studies (Meyer et al., 2018, 2020). Importantly, these compounds have shown safety and good tolerability in healthy subjects, paving the way for future robust trials involving dazucorilant in the context of AD treatment.

In conclusion, this study proves that the chronic administration of dazucorilant in J20 and 5xFAD mice effectively impedes glucocorticoid receptor-dependent pathogenic processes, along with the restoration of circulating glucocorticoid levels. This treatment, due to the extensive interaction network of glucocorticoid receptor with AD-related enzymes, results in a reduction of both amyloid and tau pathologies, ultimately leading to improved memory performance. Notably, despite a thorough analysis of several AD-related pathways following the four-week administration of dazucorilant, no undesired behavioural or biochemical side effects were observed in wild-type or transgenic animals. Finally, our findings underscore the potential superiority of dazucorilant in improving glucocorticoid receptor-mediated inflammatory processes compared to non-steroidal anti-inflammatory drugs that were ineffective in AD clinical trials (Jaturapatporn et al., 2012). Given that AD may be a stress-related disorder (Canet et al., 2019), with aberrant glucocorticoid-glucocorticoid receptor signalling playing a detrimental role in its pathophysiology, our work further emphasizes the use of selective glucocorticoid receptor modulators as a viable and potent therapeutic approach.

AUTHOR CONTRIBUTIONS

Geoffrey Canet: Conceptualization; formal analysis; investigation; methodology; validation; writing—original draft. **Charleine Zussy:** Conceptualization; formal analysis; investigation; methodology; validation; writing—original draft. **Mathieu Vitalis:** Investigation; methodology. **Françoise Morin:** Investigation; methodology. **Nathalie Chevallier:** Conceptualization; formal analysis; investigation; methodology; writing—original draft. **Hazel Hunt:** Resources; writing—original draft. **Sylvie Claeysen:** Resources; writing—original draft. **Marine Blaquière:** Investigation; methodology. **Nicola Marchi:** Conceptualization; formal analysis; methodology; validation; writing—original draft. **Emmanuel Planel:** Methodology; resources; validation; writing—original draft. **Onno C. Meijer:** Resources; validation; writing—original draft. **Catherine Desrumaux:** Methodology; resources; validation; writing—original draft. **Laurent Givalois:** Conceptualization; data curation; formal analysis; funding acquisition; investigation; methodology; project administration; resources; supervision; validation; visualization; writing—original draft.

ACKNOWLEDGEMENTS

The graphical abstract has been created with BioRender.com. The authors are thankful to Elisabeth HUETTER and the animal facility staff (CECEMA, University of Montpellier, France) for their daily assistance. They also particularly thank Corcept Therapeutics for generously providing glucocorticoid receptor ligand. Parts of this study were supported by INSERM, CNRS, University of Montpellier and EPHE annual resources (France), by a grant from 'France Alzheimer' and 'Fédération pour la Recherche sur le Cerveau' (Grant AAP SM2016#1512 - LG) and by a grant from the 'Agence Nationale de la Recherche' (ANR) under the programme 'Investissements d'Avenir' (ANR-11-LABEX-0021-LipSTIC - CD). LG, NM, CZ and MV were supported by grants from the 'Agence Nationale de la Recherche' (no. ANR-AAP2022-R22102FF-EpiNeurAge); the 'Fondation pour la Recherche Médicale' (no. MND202003011477-OPA); and the 'University of Montpellier Program of Excellence' (no. MUSE-AAP20REC-FRS09-GAiA). GC is supported by a PhD Grant from the University of Montpellier, France (CBS2 PhD programme), and by a postdoctoral fellowship from the Alzheimer Society of Canada.

CONFLICT OF INTEREST STATEMENT

HH is an employee of Corcept Therapeutics (Menlo Park, CA, USA), which develops glucocorticoid receptor ligands for clinical use. Corcept Therapeutics generously provided dazucorilant with no financial support. They are not involved in the experimental design, results analysis and conclusions of the present study. OCM receives research funding from Corcept Therapeutics. All other authors declare that they have no competing interests.

DATA AVAILABILITY STATEMENT

The data that support the findings of this study are available from the corresponding author upon reasonable request.

DECLARATION OF TRANSPARENCY AND SCIENTIFIC RIGOUR

This declaration acknowledges that this article adheres to the principles for transparent reporting and scientific rigour of preclinical studies as stated in the *BJP* guidelines for Design & Analysis, Immunoblotting and Immunohistochemistry, and Animal Experimentation, and as recommended by funding agencies, publishers and other organizations engaged with supporting research.

ORCID

Geoffrey Canet https://orcid.org/0000-0001-7291-4512
Charleine Zussy https://orcid.org/0000-0003-4945-2211
Mathieu Vitalis https://orcid.org/0009-0001-3450-9003
Françoise Morin https://orcid.org/0000-0002-8143-6644
Hazel Hunt https://orcid.org/0000-0002-4316-1301
Sylvie Claeysen https://orcid.org/0000-0002-0576-5518
Nicola Marchi https://orcid.org/0000-0001-9124-0226
Emmanuel Planel https://orcid.org/0000-0001-5128-0565
Onno C. Meijer https://orcid.org/0000-0002-8394-6859
Catherine Desrumaux https://orcid.org/0009-0004-7067-602X
Laurent Givalois https://orcid.org/0000-0002-6698-5346

REFERENCES

Alexander, S. P. H., Cidlowski, J. A., Kelly, E., Mathie, A. A., Peters, J. A., Veale, E. L., Armstrong, J. F., Faccenda, E., Harding, S. D., Davies, J. A., Coons, L., Fuller, P. J., Korach, K. S., & Young, M. J. (2023). The Concise Guide to PHARMACOLOGY 2023/24: Nuclear hormone receptors. *British Journal of Pharmacology*, *180*, S223–S240. https://doi.org/10.1111/bph.16179

Alexander, S. P. H., Fabbro, D., Kelly, E., Mathie, A. A., Peters, J. A., Veale, E. L., Armstrong, J. F., Faccenda, E., Harding, S. D., Davies, J. A., Annett, S., Boison, D., Burns, K. E., Dessauer, C., Gertsch, J., Helsby, N. A., Izzo, A. A., Ostrom, R., Papapetropoulos, A., … Wong, S. S. (2023). The Concise Guide to PHARMACOLOGY 2023/24: Enzymes. *British Journal of Pharmacology*, *180*(Suppl 2), S289–S373. https://doi.org/10.1111/bph.16181

Alexander, S. P. H., Roberts, R. E., Broughton, B. R. S., Sobey, C. G., George, C. H., Stanford, S. C., Cirino, G., Docherty, J. R., Giembycz, M. A., Hoyer, D., Insel, P. A., Izzo, A. A., Ji, Y., MacEwan, D. J., Mangum, J., Wonnacott, S., & Ahluwalia, A. (2018). Goals and practicalities of immunoblotting and immunohistochemistry: A guide for submission to the *British Journal of Pharmacology*. *British Journal of Pharmacology*, *175*, 407–411. https://doi.org/10.1111/bph.14112

Alleaume-Butaux, A., Nicot, S., Pietri, M., Baudry, A., Dakowski, C., Tixador, P., Ardila-Osorio, H., Haeberlé, A. M., Bailly, Y., Peyrin, J. M., Launay, J. M., Kellermann, O., & Schneider, B. (2015). Double-edge sword of sustained ROCK activation in prion diseases through Neuritogenesis defects and prion accumulation. *PLoS Pathogens*, *11*, e1005073. https://doi.org/10.1371/journal.ppat.1005073

Baglietto-Vargas, D., Medeiros, R., Martinez-Coria, H., LaFerla, F. M., & Green, K. N. (2013). Mifepristone alters amyloid precursor protein processing to preclude amyloid Beta and Also reduces tau pathology. *Biological Psychiatry*, *74*, 357–366. https://doi.org/10.1016/j.biopsych.2012.12.003

Baranger, K., Marchalant, Y., Bonnet, A. E., Crouzin, N., Carrete, A., Paumier, J. M., Py, N. A., Bernard, A., Bauer, C., Charrat, E., Moschke, K., Seiki, M., Vignes, M., Lichtenthaler, S. F., Checler, F., Khrestchatisky, M., & Rivera, S. (2016). MT5-MMP is a new pro-amyloidogenic proteinase that promotes amyloid pathology and cognitive decline in a transgenic mouse model of Alzheimer's disease. *Cellular and Molecular Life Sciences*, *73*, 217–236. https://doi.org/10.1007/s00018-015-1992-1

Beaudry, J. L., Dunford, E. C., Teich, T., Zaharieva, D., Hunt, H., Belanoff, J. K., & Riddell, M. C. (2014). Effects of selective and non-selective glucocorticoid receptor II antagonists on rapid-onset diabetes in young rats. *PLoS ONE*, *9*, e91248. https://doi.org/10.1371/journal.pone.0091248

Belanoff, J. K., Jurik, J., Schatzberg, L. D., DeBattista, C., & Schatzberg, A. F. (2002). Slowing the progression of cognitive decline in Alzheimer's disease using mifepristone. *Journal of Molecular Neuroscience*, *19*, 201–206. https://doi.org/10.1007/s12031-002-0033-3

Bolte, S., & Cordelières, F. P. (2006). A guided tour into subcellular colocalization analysis in light microscopy. *Journal of Microscopy*, *224*, 213–232. https://doi.org/10.1111/j.1365-2818.2006.01706.x

Borroni, B., Gardoni, F., Parnetti, L., Magno, L., Malinverno, M., Saggese, E., Calabresi, P., Spillantini, M. G., Padovani, A., & di Luca, M. (2009). Pattern of tau forms in CSF is altered in progressive supranuclear palsy. *Neurobiology of Aging*, *30*, 34–40. https://doi.org/10.1016/j.neurobiolaging.2007.05.009

Brureau, A., Zussy, C., Delair, B., Ogier, C., Ixart, G., Maurice, T., & Givalois, L. (2013). Deregulation of hypothalamic-pituitary-adrenal axis functions in an Alzheimer's disease rat model. *Neurobiology of Aging*, *34*, 1426–1439. https://doi.org/10.1016/j.neurobiolaging.2012.11.015

Canet, G., Chevallier, N., Zussy, C., Desrumaux, C., & Givalois, L. (2018). Central role of glucocorticoid receptors in Alzheimer's disease and depression. *Frontiers in Neuroscience*, *12*, 739. https://doi.org/10.3389/fnins.2018.00739

Canet, G., Hernandez, C., Zussy, C., Chevallier, N., Desrumaux, C., & Givalois, L. (2019). Is AD a stress-related disorder? Focus on the HPA Axis and its promising therapeutic targets. *Frontiers in Aging Neuroscience*, *11*, 269. https://doi.org/10.3389/fnagi.2019.00269

Canet, G., Pineau, F., Zussy, C., Hernandez, C., Hunt, H., Chevallier, N., Perrier, V., Torrent, J., Belanoff, J. K., Meijer, O. C., Desrumaux, C., & Givalois, L. (2020). Glucocorticoid receptors signaling impairment potentiates amyloid-β oligomers-induced pathology in an acute model of Alzheimer's disease. *The FASEB Journal*, *34*, 1150–1168. https://doi.org/10.1096/fj.201900723RRR

Canet, G., Rocaboy, E., Laliberté, F., Boscher, E., Guisle, I., Diego-Diaz, S., Fereydouni-Forouzandeh, P., Whittington, R. A., Hébert, S. S., Pernet, V., & Planel, E. (2023). Temperature-induced artifacts in tau phosphorylation: Implications for reliable Alzheimer's disease research. *Experimental Neurobiology*, *32*, 423–440. https://doi.org/10.5607/en23025

Canet, G., Zussy, C., Hernandez, C., Chevallier, N., Marchi, N., Desrumaux, C., & Givalois, L. (2022). Chronic glucocorticoids consumption triggers and worsens experimental Alzheimer's disease-like pathology by detrimental immune modulations. *Neuroendocrinology*, *112*, 982–997. https://doi.org/10.1159/000521559

Canet, G., Zussy, C., Hernandez, C., Maurice, T., Desrumaux, C., & Givalois, L. (2023). The pathomimetic oAβ25–35 model of Alzheimer's disease: Potential for screening of new therapeutic agents. *Pharmacology & Therapeutics*, *245*, 108398. https://doi.org/10.1016/j.pharmthera.2023.108398

Castro-Alvarez, J. F., Gutierrez-Vargas, J., Darnaudéry, M., & Cardona-Gómez, G. P. (2011). ROCK inhibition prevents tau hyperphosphorylation and p25/CDK5 increase after global cerebral ischemia. *Behavioral Neuroscience*, *125*, 465–472. https://doi.org/10.1037/a0023167

Chapman, K. E., & Seckl, J. R. (2008). 11β-HSD1, inflammation, metabolic disease and age-related cognitive (dys)function. *Neurochemical Research*, *33*, 624–636. https://doi.org/10.1007/s11064-007-9504-9

Choi, G. E., Lee, S. J., Lee, H. J., Ko, S. H., Chae, C. W., & Han, H. J. (2017). Membrane-associated effects of glucocorticoid on BACE1 upregulation and Aβ generation: Involvement of lipid raft-mediated CREB activation. *The Journal of Neuroscience*, *37*, 8459–8476. https://doi.org/10.1523/JNEUROSCI.0074-17.2017

Conze, C., Rierola, M., Trushina, N. I., Peters, M., Janning, D., Holzer, M., Heinisch, J. J., Arendt, T., Bakota, L., & Brandt, R. (2022). Caspase-cleaved tau is senescence-associated and induces a toxic gain of function by putting a brake on axonal transport. *Molecular Psychiatry*, *27*, 3010–3023. https://doi.org/10.1038/s41380-022-01538-2

Crouzin, N., Baranger, K., Cavalier, M., Marchalant, Y., Cohen-Solal, C., Roman, F. S., Khrestchatisky, M., Rivera, S., Féron, F., & Vignes, M. (2013). Area-specific alterations of synaptic plasticity in the 5XFAD

mouse model of Alzheimer's disease: Dissociation between somatosensory cortex and hippocampus. *PLoS ONE*, *8*, e74667. https://doi.org/10.1371/journal.pone.0074667

Csernansky, J. G., Dong, H. Ph.D., Fagan, A. Ph.D., Wang, L. Ph.D., Xiong, C. Ph.D., Holtzman, D. M.D., & Morris, J. M.D. (2006). Plasma cortisol and progression of dementia in subjects with Alzheimer-type dementia. *The American Journal of Psychiatry*, *163*, 2164–2169. https://doi.org/10.1176/ajp.2006.163.12.2164

Curtis, M. J., Alexander, S. P. H., Cirino, G., George, C. H., Kendall, D. A., Insel, P. A., Izzo, A. A., Ji, Y., Panettieri, R. A., Patel, H. H., Sobey, C. G., Stanford, S. C., Stanley, P., Stefanska, B., Stephens, G. J., Teixeira, M. M., Vergnolle, N., & Ahluwalia, A. (2022). Planning experiments: Updated guidance on experimental design and analysis and their reporting III. *British Journal of Pharmacology*, *179*, 3907–3913. https://doi.org/10.1111/bph.15868

David, D. J., Samuels, B. A., Rainer, Q., Wang, J. W., Marsteller, D., Mendez, I., Drew, M., Craig, D. A., Guiard, B. P., Guilloux, J. P., Artymyshyn, R. P., Gardier, A. M., Gerald, C., Antonijevic, I. A., Leonardo, E. D., & Hen, R. (2009). Neurogenesis-dependent and -independent effects of fluoxetine in an animal model of anxiety/depression. *Neuron*, *62*, 479–493. https://doi.org/10.1016/j.neuron.2009.04.017

Dávila-Bouziguet, E., Targa-Fabra, G., Ávila, J., Soriano, E., & Pascual, M. (2019). Differential accumulation of tau phosphorylated at residues Thr231, Ser262 and Thr205 in hippocampal interneurons and its modulation by tau mutations (VLW) and amyloid-β peptide. *Neurobiology of Disease*, *125*, 232–244. https://doi.org/10.1016/j.nbd.2018.12.006

De Nicola, A. F., Meyer, M., Guennoun, R., Schumacher, M., Hunt, H., Belanoff, J., de Kloet, E. R., & Gonzalez Deniselle, M. C. (2020). Insights into the therapeutic potential of glucocorticoid receptor modulators for neurodegenerative diseases. *International Journal of Molecular Sciences*, *21*(6), 2137. https://doi.org/10.3390/ijms21062137

DeWitt, D. A., Perry, G., Cohen, M., Doller, C., & Silver, J. (1998). Astrocytes regulate microglial phagocytosis of senile plaque cores of Alzheimer's disease. *Experimental Neurology*, *149*, 329–340. https://doi.org/10.1006/exnr.1997.6738

Dey, A., Hao, S., Wosiski-Kuhn, M., & Stranahan, A. M. (2017). Glucocorticoid-mediated activation of GSK3β promotes tau phosphorylation and impairs memory in type 2 diabetes. *Neurobiology of Aging*, *57*, 75–83. https://doi.org/10.1016/j.neurobiolaging.2017.05.010

Fonken, L. K., Frank, M. G., Gaudet, A. D., & Maier, S. F. (2018). Stress and aging act through common mechanisms to elicit neuroinflammatory priming. *Brain, Behavior, and Immunity*, *73*, 133–148. https://doi.org/10.1016/j.bbi.2018.07.012

Gazorpak, M., Hugentobler, K. M., Paul, D., Germain, P. L., Kretschmer, M., Ivanova, I., Frei, S., Mathis, K., Rudolf, R., Mompart Barrenechea, S., Fischer, V., Xue, X., Ptaszek, A. L., Holzinger, J., Privitera, M., Hierlemann, A., Meijer, O. C., Konrat, R., Carreira, E. M., … Gapp, K. (2023). Harnessing PROTAC technology to combat stress hormone receptor activation. *Nature Communications*, *14*, 8177. https://doi.org/10.1038/s41467-023-44031-2

Gentenaar, M., Meulmeester, F. L., van der Burg, X. R., Hoekstra, A. T., Hunt, H., Kroon, J., van Roon-Mom, W. M. C., & Meijer, O. C. (2024). Glucocorticoid receptor antagonist CORT113176 attenuates motor and neuropathological symptoms of Huntington's disease in R6/2 mice. *Experimental Neurology*, *374*, 114675. https://doi.org/10.1016/j.expneurol.2024.114675

Giannoni, P., Arango-Lievano, M., Neves, I. D., Rousset, M. C., Baranger, K., Rivera, S., Jeanneteau, F., Claeysen, S., & Marchi, N. (2016). Cerebrovascular pathology during the progression of experimental Alzheimer's disease. *Neurobiology of Disease*, *88*, 107–117. https://doi.org/10.1016/j.nbd.2016.01.001

Green, K. N., Billings, L. M., Roozendaal, B., McGaugh, J. L., & LaFerla, F. M. (2006). Glucocorticoids increase amyloid-beta and tau pathology in a mouse model of Alzheimer's disease. *The Journal of Neuroscience*, *26*, 9047–9056. https://doi.org/10.1523/JNEUROSCI.2797-06.2006

Groeneweg, F. L., Karst, H., de Kloet, E. R., & Joëls, M. (2011). Rapid non-genomic effects of corticosteroids and their role in the central stress response. *The Journal of Endocrinology*, *209*, 153–167.

Hamano, T., Yen, S.-H., Gendron, T., Ko, L., & Kuriyama, M. (2012). Pitavastatin decreases tau levels via the inactivation of rho/ROCK. *Neurobiology of Aging*, *33*, 2306–2320. https://doi.org/10.1016/j.neurobiolaging.2011.10.020

Hansen, D. V., Hanson, J. E., & Sheng, M. (2018). Microglia in Alzheimer's disease. *Journal of Cell Biology*, *217*, 459–472. https://doi.org/10.1083/jcb.201709069

Hartmann, A., Veldhuis, J. D., Deuschle, M., Standhardt, H., & Heuser, I. (1997). Twenty-four hour cortisol release profiles in patients with Alzheimer's and Parkinson's disease compared to Normal controls: Ultradian secretory Pulsatility and diurnal variation. *Neurobiology of Aging*, *18*, 285–289. https://doi.org/10.1016/S0197-4580(97)80309-0

Henderson, B. W., Gentry, E. G., Rush, T., Troncoso, J. C., Thambisetty, M., Montine, T. J., & Herskowitz, J. H. (2016). Rho-associated protein kinase 1 (ROCK1) is increased in Alzheimer's disease and ROCK1 depletion reduces amyloid-β levels in brain. *Journal of Neurochemistry*, *138*, 525–531. https://doi.org/10.1111/jnc.13688

Herbert, J., & Lucassen, P. J. (2016). Depression as a risk factor for Alzheimer's disease: Genes, steroids, cytokines and neurogenesis - what do we need to know? *Frontiers in Neuroendocrinology*, *41*, 153–171. https://doi.org/10.1016/j.yfrne.2015.12.001

Hess, S. E., Rohr, S., Dufour, B. D., Gaskill, B. N., Pajor, E. A., & Garner, J. P. (2008). Home improvement: C57BL/6J mice given more naturalistic nesting materials build better nests. *Journal of the American Association for Laboratory Animal Science*, *47*, 25–31.

Hong, D.-H., & Forsberg, N. E. (1995). Effects of dexamethasone on protein degradation and protease gene expression in rat L8 myotube cultures. *Molecular and Cellular Endocrinology*, *108*, 199–209. https://doi.org/10.1016/0303-7207(95)03476-N

Hoogendijk, W. J. G., Meynen, G., Endert, E., Hofman, M. A., & Swaab, D. F. (2006). Increased cerebrospinal fluid cortisol level in Alzheimer's disease is not related to depression. *Neurobiology of Aging*, *27*(5), 780.e1–780.e2. https://doi.org/10.1016/j.neurobiolaging.2005.07.017

Iqbal, K., Grundke-Iqbal, I., Smith, A. J., George, L., Tung, Y. C., & Zaidi, T. (1989). Identification and localization of a tau peptide to paired helical filaments of Alzheimer disease. *Proceedings. National Academy of Sciences. United States of America*, *86*, 5646–5650. https://doi.org/10.1073/pnas.86.14.5646

Jankord, R., & Herman, J. P. (2008). Limbic regulation of hypothalamo-pituitary-adrenocortical function during acute and chronic stress. *Annals of the New York Academy of Sciences*, *1148*, 64–73. https://doi.org/10.1196/annals.1410.012

Jaturapatporn, D., Isaac, M. G. E. K. N., McCleery, J., & Tabet, N. (2012). Aspirin, steroidal and non-steroidal anti-inflammatory drugs for the treatment of Alzheimer's disease. *Cochrane Database of Systematic Reviews*, *2012*, CD006378. https://doi.org/10.1002/14651858.CD006378.pub2

Jay, T. R., Miller, C. M., Cheng, P. J., Graham, L. C., Bemiller, S., Broihier, M. L., Xu, G., Margevicius, D., Karlo, J. C., Sousa, G. L., Cotleur, A. C., Butovsky, O., Bekris, L., Staugaitis, S. M., Leverenz, J. B., Pimplikar, S. W., Landreth, G. E., Howell, G. R., Ransohoff, R. M., & Lamb, B. T. (2015). TREM2 deficiency eliminates TREM2+ inflammatory macrophages and ameliorates pathology in Alzheimer's disease mouse models. *Journal of Experimental Medicine*, *212*, 287–295. https://doi.org/10.1084/jem.20142322

Jin, N., Yin, X., Yu, D., Cao, M., Gong, C. X., Iqbal, K., Ding, F., Gu, X., & Liu, F. (2015). Truncation and activation of GSK-3β by calpain I: A molecular mechanism links to tau hyperphosphorylation in Alzheimer's

disease. *Scientific Reports*, *5*, 8187. https://doi.org/10.1038/srep08187

Jozic, I., Vukelic, S., Stojadinovic, O., Liang, L., Ramirez, H. A., Pastar, I., & Tomic Canic, M. (2017). Stress signals, mediated by membranous glucocorticoid receptor, activate PLC/PKC/GSK-3β/β-catenin pathway to inhibit wound closure. *Journal of Investigative Dermatology*, *137*, 1144–1154. https://doi.org/10.1016/j.jid.2016.11.036

Kobayashi, Y., Mercado, N., Barnes, P. J., & Ito, K. (2011). Defects of protein phosphatase 2A causes corticosteroid insensitivity in severe asthma. *PLoS ONE*, *6*, e27627. https://doi.org/10.1371/journal.pone.0027627

Lahiri, D. K. (2004). Functional characterization of amyloid beta precursor protein regulatory elements: Rationale for the identification of genetic polymorphism. *Annals of the New York Academy of Sciences*, *1030*, 282–288. https://doi.org/10.1196/annals.1329.035

Lee, M. S., Kwon, Y. T., Li, M., Peng, J., Friedlander, R. M., & Tsai, L. H. (2000). Neurotoxicity induces cleavage of p35 to p25 by calpain. *Nature*, *405*, 360–364. https://doi.org/10.1038/35012636

Leng, F., & Edison, P. (2021). Neuroinflammation and microglial activation in Alzheimer disease: Where do we go from here? *Nature Reviews. Neurology*, *17*, 157–172. https://doi.org/10.1038/s41582-020-00435-y

Lesort, M., Jope, R. S., & Johnson, G. V. (1999). Insulin transiently increases tau phosphorylation: Involvement of glycogen synthase kinase-3beta and Fyn tyrosine kinase. *Journal of Neurochemistry*, *72*, 576–584. https://doi.org/10.1046/j.1471-4159.1999.0720576.x

Li, X. H., Liu, N. B., Zhang, M. H., Zhou, Y. L., Liao, J. W., Liu, X. Q., & Chen, H. W. (2007). Effects of chronic multiple stress on learning and memory and the expression of Fyn, BDNF, TrkB in the hippocampus of rats. *Chinese Medical Journal*, *120*, 669–674. https://doi.org/10.1097/00029330-200704020-00011

Liddelow, S. A., Guttenplan, K. A., Clarke, L. E., Bennett, F. C., Bohlen, C. J., Schirmer, L., Bennett, M. L., Münch, A. E., Chung, W. S., Peterson, T. C., Wilton, D. K., Frouin, A., Napier, B. A., Panicker, N., Kumar, M., Buckwalter, M. S., Rowitch, D. H., Dawson, V. L., Dawson, T. M., … Barres, B. A. (2017). Neurotoxic reactive astrocytes are induced by activated microglia. *Nature*, *541*, 481–487. https://doi.org/10.1038/nature21029

Lilley, E., Stanford, S. C., Kendall, D. E., Alexander, S. P. H., Cirino, G., Docherty, J. R., George, C. H., Insel, P. A., Izzo, A. A., Ji, Y., Panettieri, R. A., Sobey, C. G., Stefanska, B., Stephens, G., Teixeira, M., & Ahluwalia, A. (2020). ARRIVE 2.0 and the British Journal of Pharmacology: Updated guidance for 2020. *British Journal of Pharmacology*, *177*(16), 3611–3616. https://doi.org/10.1111/BPH.15178

Liu, Y., Su, Y., Sun, S., Wang, T., Qiao, X., Run, X., & Liang, Z. (2012). Tau phosphorylation and μ-calpain activation mediate the dexamethasone-induced inhibition on the insulin-stimulated Akt phosphorylation. *PLoS ONE*, *7*, e35783. https://doi.org/10.1371/journal.pone.0035783

Löwenberg, M., Tuynman, J., Bilderbeek, J., Gaber, T., Buttgereit, F., van, S., Peppelenbosch, M., & Hommes, D. (2005). Rapid immunosuppressive effects of glucocorticoids mediated through Lck and Fyn. *Blood*, *106*, 1703–1710. https://doi.org/10.1182/blood-2004-12-4790

Lv, Z., Hu, M., Ren, X., Fan, M., Zhen, J., Chen, L., Lin, J., Ding, N., Wang, Q., & Wang, R. (2016). Fyn mediates high glucose-induced actin cytoskeleton reorganization of podocytes via promoting ROCK activation *in vitro*. *Journal of Diabetes Research*, *2016*, 5671803. https://doi.org/10.1155/2016/5671803

Manders, E. M. M., Stap, J., Brakenhoff, G. J., Driel, R. V., & Aten, J. A. (1992). Dynamics of three-dimensional replication patterns during the s-phase, analysed by double labelling of dna and confocal microscopy. *Journal of Cell Science*, *103*, 857–862. https://doi.org/10.1242/jcs.103.3.857

Mansuy, M., Baille, S., Canet, G., Borie, A., Cohen-Solal, C., Vignes, M., Perrier, V., Chevallier, N., le Guern, N., Deckert, V., Lagrost, L., Givalois, L., & Desrumaux, C. (2018). Deletion of plasma phospholipid transfer protein (PLTP) increases microglial phagocytosis and reduces cerebral amyloid-β deposition in the J20 mouse model of Alzheimer's disease. *Oncotarget*, *9*, 19688–19703. https://doi.org/10.18632/oncotarget.24802

Martin, L., Latypova, X., Wilson, C. M., Magnaudeix, A., Perrin, M. L., & Terro, F. (2013). Tau protein phosphatases in Alzheimer's disease: The leading role of PP2A. *Ageing Research Reviews*, *12*, 39–49. https://doi.org/10.1016/j.arr.2012.06.008

Martin, L., Latypova, X., Wilson, C. M., Magnaudeix, A., Perrin, M. L., Yardin, C., & Terro, F. (2013). Tau protein kinases: Involvement in Alzheimer's disease. *Ageing Research Reviews*, *12*, 289–309. https://doi.org/10.1016/j.arr.2012.06.003

McEwen, B. S. (2008). Central effects of stress hormones in health and disease: Understanding the protective and damaging effects of stress and stress mediators. *European Journal of Pharmacology*, *583*, 174–185. https://doi.org/10.1016/j.ejphar.2007.11.071

Meijer, O. C., Koorneef, L. L., & Kroon, J. (2018). Glucocorticoid receptor modulators. *Annales d'Endocrinologie*, *79*, 107–111. https://doi.org/10.1016/j.ando.2018.03.004

Mejía, S., Giraldo, M., Pineda, D., Ardila, A., & Lopera, F. (2003). Nongenetic factors as modifiers of the age of onset of familial Alzheimer's disease. *International Psychogeriatrics*, *15*, 337–349. https://doi.org/10.1017/S1041610203009591

Meyer, M., Kruse, M. S., Garay, L., Lima, A., Roig, P., Hunt, H., Belanoff, J., de Kloet, E. R., Deniselle, M. C. G., & de Nicola, A. F. (2020). Long-term effects of the glucocorticoid receptor modulator CORT113176 in murine motoneuron degeneration. *Brain Research*, *1727*, 146551. https://doi.org/10.1016/j.brainres.2019.146551

Meyer, M., Lara, A., Hunt, H., Belanoff, J., de Kloet, E. R., Gonzalez Deniselle, M. C., & de Nicola, A. F. (2018). The selective glucocorticoid receptor modulator Cort 113176 reduces neurodegeneration and Neuroinflammation in wobbler mice spinal cord. *Neuroscience*, *384*, 384–396. https://doi.org/10.1016/j.neuroscience.2018.05.042

Mucke, L., Masliah, E., Yu, G. Q., Mallory, M., Rockenstein, E. M., Tatsuno, G., Hu, K., Kholodenko, D., Johnson-Wood, K., & McConlogue, L. (2000). High-level neuronal expression of abeta 1-42 in wild-type human amyloid protein precursor transgenic mice: Synaptotoxicity without plaque formation. *The Journal of Neuroscience*, *20*, 4050–4058. https://doi.org/10.1523/JNEUROSCI.20-11-04050.2000

Oakley, H., Cole, S. L., Logan, S., Maus, E., Shao, P., Craft, J., Guillozet-Bongaarts, A., Ohno, M., Disterhoft, J., van Eldik, L., Berry, R., & Vassar, R. (2006). Intraneuronal β-amyloid aggregates, neurodegeneration, and neuron loss in transgenic mice with five familial Alzheimer's disease mutations: Potential factors in amyloid plaque formation. *The Journal of Neuroscience*, *26*, 10129–10140. https://doi.org/10.1523/JNEUROSCI.1202-06.2006

Oliveira Monteiro, M. P. A., Salheb Oliveira, D. S. M., Manzine, P. R., Crispim Nascimento, C. M., dos Santos Orlandi, A. A., de Oliveira Gomes, G. A., dos Santos Orlandi, F., Zazzetta, M. S., Pott-Junior, H., & Cominetti, M. R. (2021). ADAM10 plasma levels predict worsening in cognition of older adults: A 3-year follow-up study. *Alzheimer's Research & Therapy*, *13*, 18. https://doi.org/10.1186/s13195-020-00750-y

Paliogianni, F., Hama, N., Balow, J. E., Valentine, M. A., & Boumpas, D. T. (1995). Glucocorticoid-mediated regulation of protein phosphorylation in primary human T cells. Evidence for induction of phosphatase activity. *Journal of Immunology*, *155*, 1809–1817. https://doi.org/10.4049/jimmunol.155.4.1809

Panettieri, R. A., Schaafsma, D., Amrani, Y., Koziol-White, C., Ostrom, R., & Tliba, O. (2019). Non-genomic effects of glucocorticoids: An updated

view. *Trends in Pharmacological Sciences*, *40*, 38–49. https://doi.org/10.1016/j.tips.2018.11.002

Percie du Sert, N., Hurst, V., Ahluwalia, A., Alam, S., Avey, M. T., Baker, M., Browne, W. J., Clark, A., Cuthill, I. C., Dirnagl, U., Emerson, M., Garner, P., Holgate, S. T., Howells, D. W., Karp, N. A., Lazic, S. E., Lidster, K., MacCallum, C. J., Macleod, M., … Würbel, H. (2020). The ARRIVE guidelines 2.0: Updated guidelines for reporting animal research. *PLoS Biology*, *18*, e3000410. https://doi.org/10.1371/journal.pbio.3000410

Perretti, M., & D'Acquisto, F. (2009). Annexin A1 and glucocorticoids as effectors of the resolution of inflammation. *Nature Reviews. Immunology*, *9*, 62–70. https://doi.org/10.1038/nri2470

Petta, I., Dejager, L., Ballegeer, M., Lievens, S., Tavernier, J., de Bosscher, K., & Libert, C. (2016). The Interactome of the glucocorticoid receptor and its influence on the actions of glucocorticoids in combatting inflammatory and infectious diseases. *Microbiology and Molecular Biology Reviews*, *80*, 495–522. https://doi.org/10.1128/MMBR.00064-15

Pineau, F., Canet, G., Desrumaux, C., Hunt, H., Chevallier, N., Ollivier, M., Belanoff, J. K., & Givalois, L. (2016). New selective glucocorticoid receptor modulators reverse amyloid-β peptide-induced hippocampus toxicity. *Neurobiology of Aging*, *45*, 109–122. https://doi.org/10.1016/j.neurobiolaging.2016.05.018

Plouffe, V., Mohamed, N. V., Rivest-McGraw, J., Bertrand, J., Lauzon, M., & Leclerc, N. (2012). Hyperphosphorylation and cleavage at D421 enhance tau secretion. *PLoS ONE*, *7*, e36873. https://doi.org/10.1371/journal.pone.0036873

Price, B. R., Sudduth, T. L., Weekman, E. M., Johnson, S., Hawthorne, D., Woolums, A., & Wilcock, D. M. (2020). Therapeutic Trem2 activation ameliorates amyloid-beta deposition and improves cognition in the 5XFAD model of amyloid deposition. *Journal of Neuroinflammation*, *17*, 238. https://doi.org/10.1186/s12974-020-01915-0

Quan, Q., Qian, Y., Li, X., & Li, M. (2019). CDK5 participates in amyloid-β production by regulating PPARγ phosphorylation in primary rat hippocampal neurons. *JAD*, *71*, 443–460. https://doi.org/10.3233/JAD-190026

Querfurth, H. W., & LaFerla, F. M. (2010). Alzheimer's disease. *The New England Journal of Medicine*, *362*, 329–344. https://doi.org/10.1056/NEJMra0909142

Reul, J. M., & de Kloet, E. R. (1985). Two receptor systems for corticosterone in rat brain: Microdistribution and differential occupation. *Endocrinology*, *117*, 2505–2511. https://doi.org/10.1210/endo-117-6-2505

Ries, M., Loiola, R., Shah, U. N., Gentleman, S. M., Solito, E., & Sastre, M. (2016). The anti-inflammatory Annexin A1 induces the clearance and degradation of the amyloid-β peptide. *Journal of Neuroinflammation*, *13*, 234. https://doi.org/10.1186/s12974-016-0692-6

Rochais, C., Lecoutey, C., Hamidouche, K., Giannoni, P., Gaven, F., Cem, E., Mignani, S., Baranger, K., Freret, T., Bockaert, J., Rivera, S., Boulouard, M., Dallemagne, P., & Claeysen, S. (2020). Donecopride, a Swiss army knife with potential against Alzheimer's disease. *British Journal of Pharmacology*, *177*, 1988–2005. https://doi.org/10.1111/bph.14964

Roozendaal, B. (2000). 1999 Curt P. Richter award. Glucocorticoids and the regulation of memory consolidation. *Psychoneuroendocrinology*, *25*, 213–238. https://doi.org/10.1016/S0306-4530(99)00058-X

Rothman, S. M., Herdener, N., Camandola, S., Texel, S. J., Mughal, M. R., Cong, W. N., Martin, B., & Mattson, M. P. (2012). 3xTgAD mice exhibit altered behavior and elevated Aβ after chronic mild social stress. *Neurobiology of Aging*, *33*(4), 830.e1–830.e12. https://doi.org/10.1016/j.neurobiolaging.2011.07.005

Rubenstein, N. M., Callahan, J. A., Lo, D. H., & Firestone, G. L. (2007). Selective glucocorticoid control of rho kinase isoforms regulate cell-cell interactions. *Biochemical and Biophysical Research Communications*, *354*, 603–607. https://doi.org/10.1016/j.bbrc.2007.01.024

Sambamurti, K., Kinsey, R., Maloney, B., Ge, Y.-W., & Lahiri, D. K. (2004). Gene structure and organization of the human beta-secretase (BACE) promoter. *The FASEB Journal*, *18*, 1034–1036. https://doi.org/10.1096/fj.03-1378fje

Scales, T. M., Derkinderen, P., Leung, K. Y., Byers, H. L., Ward, M. A., Price, C., Bird, I. N., Perera, T., Kellie, S., Williamson, R., Anderton, B. H., & Reynolds, C. H. (2011). Tyrosine phosphorylation of tau by the Src family kinases Lck and Fyn. *Molecular Neurodegeneration*, *6*, 12. https://doi.org/10.1186/1750-1326-6-12

Selkoe, D. J., & Hardy, J. (2016). The amyloid hypothesis of Alzheimer's disease at 25 years. *EMBO Molecular Medicine*, *8*, 595–608. https://doi.org/10.15252/emmm.201606210

Sengupta, A., Kabat, J., Novak, M., Wu, Q., Grundke-Iqbal, I., & Iqbal, K. (1998). Phosphorylation of tau at both Thr 231 and Ser 262 is required for maximal inhibition of its binding to microtubules. *Archives of Biochemistry and Biophysics*, *357*, 299–309. https://doi.org/10.1006/abbi.1998.0813

Sivakumaran, M. H., Mackenzie, A. K., Callan, I. R., Ainge, J. A., & O'Connor, A. R. (2018). The discrimination ratio derived from novel object recognition tasks as a measure of recognition memory sensitivity, not bias. *Scientific Reports*, *8*, 11579. https://doi.org/10.1038/s41598-018-30030-7

Söllvander, S., Nikitidou, E., Brolin, R., Söderberg, L., Sehlin, D., Lannfelt, L., & Erlandsson, A. (2016). Accumulation of amyloid-β by astrocytes result in enlarged endosomes and microvesicle-induced apoptosis of neurons. *Molecular Neurodegeneration*, *11*, 38. https://doi.org/10.1186/s13024-016-0098-z

Sugimoto, M. A., Vago, J. P., Teixeira, M. M., & Sousa, L. P. (2016). Annexin A1 and the resolution of inflammation: Modulation of neutrophil recruitment, apoptosis, and clearance. *Journal of Immunology Research*, *2016*, 8239258. https://doi.org/10.1155/2016/8239258

Sundahl, N., Bridelance, J., Libert, C., De Bosscher, K., & Beck, I. M. (2015). Selective glucocorticoid receptor modulation: New directions with non-steroidal scaffolds. *Pharmacology & Therapeutics*, *152*, 28–41. https://doi.org/10.1016/j.pharmthera.2015.05.001

Timmermans, S., Souffriau, J., & Libert, C. (2019). A general introduction to glucocorticoid biology. *Frontiers in Immunology*, *10*, 1545. https://doi.org/10.3389/fimmu.2019.01545

Viho, E., Buurstede, J., Mahfouz, A., Koorneef, L., van, L., Houtman, R., Hunt, H., Kroon, J., & Meijer, O. (2019). Corticosteroid action in the brain: The potential of selective receptor modulation. *Neuroendocrinology*, *109*, 266–276. https://doi.org/10.1159/000499659

Wang, Y., Ulland, T. K., Ulrich, J. D., Song, W., Tzaferis, J. A., Hole, J. T., Yuan, P., Mahan, T. E., Shi, Y., Gilfillan, S., Cella, M., Grutzendler, J., DeMattos, R. B., Cirrito, J. R., Holtzman, D. M., & Colonna, M. (2016). TREM2-mediated early microglial response limits diffusion and toxicity of amyloid plaques. *Journal of Experimental Medicine*, *213*, 667–675. https://doi.org/10.1084/jem.20151948

Zhang, Y., Leung, D. Y. M., Nordeen, S. K., & Goleva, E. (2009). Estrogen inhibits glucocorticoid action via protein phosphatase 5 (PP5)-mediated glucocorticoid receptor dephosphorylation. *The Journal of Biological Chemistry*, *284*, 24542–24552. https://doi.org/10.1074/jbc.M109.021469

Zheng-Fischhöfer, Q., Biernat, J., Mandelkow, E. M., Illenberger, S., Godemann, R., & Mandelkow, E. (1998). Sequential phosphorylation of tau by glycogen synthase kinase-3β and protein kinase a at Thr212 and Ser214 generates the Alzheimer-specific epitope of antibody AT100 and requires a paired-helical-filament-like conformation. *European Journal of Biochemistry*, *252*, 542–552. https://doi.org/10.1046/j.1432-1327.1998.2520542.x

Zhuravleva, V., Vaz-Silva, J., Zhu, M., Gomes, P., Silva, J. M., Sousa, N., Sotiropoulos, I., & Waites, C. L. (2021). Rab35 and glucocorticoids regulate APP and BACE1 trafficking to modulate Aβ production. *Cell Death & Disease*, *12*, 1137. https://doi.org/10.1038/s41419-021-04433-w

Zub, E., Canet, G., Garbelli, R., Blaquiere, M., Rossini, L., Pastori, C., Sheikh, M., Reutelingsperger, C., Klement, W., de Bock, F., Audinat, E., Givalois, L., Solito, E., & Marchi, N. (2019). The GR-ANXA1 pathway is a pathological player and a candidate target in epilepsy. *The FASEB Journal*, *33*, 13998–14009. https://doi.org/10.1096/fj.201901596R

Zussy, C., Brureau, A., Delair, B., Marchal, S., Keller, E., Ixart, G., Naert, G., Meunier, J., Chevallier, N., Maurice, T., & Givalois, L. (2011). Time-course and regional analyses of the physiopathological changes induced after cerebral injection of an amyloid β fragment in rats. *The American Journal of Pathology*, *179*, 315–334. https://doi.org/10.1016/j.ajpath.2011.03.021

Zussy, C., Brureau, A., Keller, E., Marchal, S., Blayo, C., Delair, B., Ixart, G., Maurice, T., & Givalois, L. (2013). Alzheimer's disease related markers, cellular toxicity and behavioral deficits induced six weeks after oligomeric amyloid-β peptide injection in rats. *PLoS ONE*, *8*, e53117. https://doi.org/10.1371/journal.pone.0053117

Zussy, C., John, R., Urgin, T., Otaegui, L., Vigor, C., Acar, N., Canet, G., Vitalis, M., Morin, F., Planel, E., Oger, C., Durand, T., Rajshree, S. L., Givalois, L., Devarajan, P. V., & Desrumaux, C. (2022). Intranasal Administration of Nanovectorized Docosahexaenoic Acid (DHA) improves cognitive function in two complementary mouse models of Alzheimer's disease. *Antioxidants*, *11*, 838. https://doi.org/10.3390/antiox11050838

SUPPORTING INFORMATION

Additional supporting information can be found online in the Supporting Information section at the end of this article.

How to cite this article: Canet, G., Zussy, C., Vitalis, M., Morin, F., Chevallier, N., Hunt, H., Claeysen, S., Blaquière, M., Marchi, N., Planel, E., Meijer, O. C., Desrumaux, C., & Givalois, L. (2025). Advancing Alzheimer's disease pharmacotherapy: efficacy of glucocorticoid modulation with dazucorilant (CORT113176) in preclinical mouse models. *British Journal of Pharmacology*, *182*(9), 1930–1956. https://doi.org/10.1111/bph.17457